Division of Cardiology, Department of Medicine
Helsinki University Central Hospital
Helsinki, Finland

Electrocardiographic repolarization variables in detecting myocardial infarction and ischemic injury

From body surface potential mapping to a single lead

Paula Vesterinen

ACADEMIC DISSERTATION
To be publicly discussed, by the permission of the Medical Faculty of the University of Helsinki, in Auditorium 2 of the Meilahti Hospital, on October 19, 2007, at 12 o'clock noon.
Helsinki 2007

Supervised by:

Docent Lauri Toivonen, M.D., Ph.D.
Division of Cardiology, Department of Medicine
Helsinki University Central Hospital
Helsinki, Finland

Docent Markku Mäkijärvi, M.D., Ph.D
Division of Cardiology, Department of Medicine
Helsinki University Central Hospital
Helsinki, Finland

Reviewed by:

Professor Mikael Dellborg, M.D., Ph.D.
Sahlgrenska University Hospital
University of Gothenburg
Göteborg, Sweden

Professor Jari Hyttinen, D.Sc.(Tech.)
Ragnar Granit Insititute
Tampere University of Technology
Tampere, Finland

ISBN 978-952-92-2563-7 (pbk.)
ISBN 978-952-10-4107-5 (PDF)
Helsinki University Printing House
Helsinki 2007

To Tuure, Reko and Lalli

CONTENTS

LIST OF ORIGINAL PUBLICATIONS 7

ABBREVIATIONS 8

ABSTRACT 9

1 INTRODUCTION 11

2 REVIEW OF THE LITERATURE 13

2.1 Electrophysiology of depolarization 13

2.2 Electrophysiology of repolarization 13

2.2.1 Transmural gradient of repolarization 13

2.2.2 Transventricular gradient of repolarization 14

2.3 Ventricular gradient 16

2.4 Clinical applications of the depolarization, the repolarization, and the ventricular gradients 17

2.5 Electrophysiology of the ischemic myocardial tissue 19

2.6 The standard 12-lead ECG in diagnosing myocardial infarction 22

2.6.1 Prior MI 22

2.6.2 Coding systems for myocardial infarction 23

2.6.2.1 The Minnesota code 23

2.6.2.2 The Selvester score 23

2.6.2.3 The Cardiac Infarction Injury score 23

2.6.2.4 The Washington code 24

2.6.2.5 The Punsar code 24

2.6.2.6 The Novacode 24

2.6.3 Acute MI 25

2.6.4 Q wave and non-Q-wave myocardial infarction 28

2.6.5 ST-segment elevation and ST-segment depression myocardial ischemia 30

2.6.6 Evolution of ECG changes after myocardial infarction 32
2.7 Body surface potential mapping (BSPM) 33
2.7.1 Distribution of BSPM variables in healthy subjects 34
2.7.2 BSPM in prior MI 34
2.7.3 BSPM in acute ischemia 35
2.7.4 Optimal recording locations for detecting myocardial ischaemia 38
2.7.5 Optimal recording locations for detecting myocardial infarction scar 39
3 AIMS OF THE STUDY 40
4 MATERIALS AND METHODS 41
4.1 Study subjects 41
4.1.1 Studies I and II 41
4.1.2 Studies III, IV, and V 42
4.1.3 Study VI 43
4.2 BSPM recording and data processing 44
4.3 Discriminant index analysis 46
4.4 Map display 47
4.5 Statistical analysis 47
5 RESULTS OF THE STUDIES 48
5.1 Diagnostic performance of the electrocardiographic variables 48
5.1.1 QRS segment time integrals: sextiles and quartiles (I, IV, V, VI) 48
5.1.2 QRS and STT time integrals (II, III, IV,V) 51
5.1.3 Spatial correlation of the QRS and STT time integrals (II, III, V, VI) 52
5.1.4 QRSSTT time integral and the T maximum amplitude in prior MI (IV, V) 54
5.1.5 QRSSTT time integral and the T maximum amplitude in evolving ischemic myocardial injury (VI) 57
6 DISCUSSION 60

6.1 Main findings 60

6.2 MI and the ventricular gradient 60

6.3 Performance of the ECG variables according to MI location 61

6.4 Contribution to previous studies 62

6.5 Study limitations 64

6.6 Clinical implications 64

7 CONCLUSIONS 65

ACKNOWLEDGEMENTS 66

REFERENCES 69

LIST OF ORIGINAL PUBLICATIONS

This thesis is based on the following publications:

I Vesterinen P, Hänninen H, Karvonen M, Lauerma K, Holmström M, Mäkijärvi M, Väänänen H, Nenonen J, Katila T, Toivonen L. Temporal Analysis of the Depolarization Wave of Healed Myocardial Infarction in Body Surface Potential Mapping. Ann Noninvas Electro, 9, 234-42, 2004.

II Vesterinen P, Hänninen H, Karvonen M, Lauerma K, Holmström M, Mäkijärvi M, Väänänen H, Stenroos M, Nenonen J, Katila T, Toivonen L. Spatial Repolarization Abnormalities in Old Myocardial Infarction. J Electrocardiol, 38, 264-70, 2005.

III Vesterinen P, Hänninen H, Stenroos M, Korhonen P, Husa T, Tierala I, Väänänen H, Toivonen L. Spatial inversion of depolarization and repolarization waves in body surface potential mapping as indicator of old myocardial infarction. Lect Notes Comput Sc 3504, Springer 2005; 278-282.

IV Vesterinen P, Väänänen H, Hänninen H, Korhonen P, Tierala I, Husa T, Mäkijärvi M, Toivonen L. Single-lead electrocardiographic variables in the detection of prior myocardial infarction with respect to Q-wave status and infarct age. Cardiology, in press.

V Vesterinen P, Väänänen H, Stenroos M, Hänninen H, Korhonen P, Tierala I, Husa T, Mäkijärvi M, Toivonen L. Detection and localisation of prior myocardial infarction by repolarisation variables in optimal body-surface locations. Int J Cardiol, in press.

VI Vesterinen P, Lindholm M, Kylmälä M, Dabek J, Konttila T, Vaananen H, Stenroos M, Tierala I, Hänninen H, Oikarinen L, Mäkijärvi M, Nieminen MS, Toivonen L. QT integral, a single-lead variable for the automatic detection of acute myocardial ischemia. Submitted.

The studies are referred to in the text by their roman numerals. The original publications are reprinted with the permission of the copyright holders.

ABBREVIATIONS

ACS	acute coronary syndrome
AP	action potential
APD	action potential duration
AT	activation time
AUC	area under receiver operating characteristic curve
BSPM	body surface potential mapping
CCU	coronary care unit
CE-CMR	contrast-enhanced cardiac magnetic resonance
CE-MRI	contrast-enhanced magnetic resonance imaging (Study I)
CHD	coronary heart disease
DI	discriminant index
ECG	electrocardiogram
ED	emergency department
LAD	left anterior descending coronary artery
LCX	left circumflex coronary artery
LV	left ventricle
LVEF	left ventricular ejection fraction
LVH	left ventricular hypertrophy
MAP	monophasic action potential
MI	myocardial infarction
NQMI	non-Q-wave myocardial infarction
NSTEMI	non-ST-elevation acute myocardial infarction
QRSSTT integral	time-voltage integral from the onset of the QRS to the end of the T-wave (Studys II-V)
QT integral	time-voltage integral from the onset of the QRS to the end of the T-wave (Study VI)
QMI	Q-wave myocardial infarction
RCA	right coronary artery
ROC	receiver operating characteristic
RT	repolarization time
STEMI	ST-elevation acute myocardial infarction
TCRT	total cosine between R and T
TWR	T-wave residuum
UAP	unstable angina pectoris

ABSTRACT

The aim of the studies included in this thesis was to improve the relatively poor diagnostic capability of electrocardiography (ECG) in detecting myocardial ischemic injury with a future goal of an automatic screening and monitoring method for ischemic heart disease.

The method of choice in the studies was body surface potential mapping (BSPM), containing numerous leads, with intention to find the optimal recording sites. Resting BSPM registrations were examined to find the optimal recording locations and optimal ECG variables for ischemia and myocardial infarction (MI) diagnostics.

The studies included 144 patients with prior MI, 79 patients with evolving ischemia, 42 patients with left ventricular hypertrophy (LVH) and 84 healthy controls. In the studies I and II the same study subject population of 24 patients and 24 controls was examined. In study I the foci of interest were the prior MI induced changes in the depolarization wave and its time segments with respect to MI location, verified by contrast enhanced magnetic resonance imaging (CE-CMR). Study II examined the depolarization and repolarization waves in prior MI detection, with respect to the Minnesota code Q-wave status and in relation to each other. Studies III-V examined 144 patients with prior MI, including those in studies I and II. In study III the spatial characteristics of the depolarization and repolarization waves and their mutual relation in prior MI was of interest. In study IV depolarization and repolarization variables were examined with respect to time elapsed from MI and to the Minnesota code Q-wave status and in study V with respect to MI location. In study VI the depolarization and repolarization variables were studied in 79 patients in the face of evolving myocardial ischemia and ischemic injury.

When analyzed from a single lead at any recording site the results revealed superiority of the repolarization variables over the depolarization variables and over the conventional 12-lead ECG methods, both in the detection of prior MI and evolving ischemic injury. The repolarization variables, with an emphasis on the QT integral covering both depolarization and repolarization, appeared indifferent to the Q-wave status, the time elapsed from MI, or the MI or ischemia location. In the face of evolving ischemic injury the performance of the QT integral was not hampered even by underlying LVH. The depolarization variables were affected by MI location, MI size, and the Q-wave status. The examined depolarization and repolarization variables were effective when recorded in a single site, in contrast to the more complex 12-lead ECG criteria of prior MI or acute ischemia. The inverse spatial correlation of the depolarization and depolarization waves in myocardial ischemia and injury could be reduced into the QT integral variable recorded in a single site.

In conclusion, the QT integral variable, detectable in a single lead, with optimal recording site on the left flank, was able to detect prior MI and evolving ischemic injury more effectively than the conventional ECG markers. The QT integral, in a single-lead or a small number of leads, offers potential for automated screening of ischemic heart disease, acute ischemia monitoring and therapeutic decision-guiding as well as risk stratification.

1 INTRODUCTION

Electrocardiography has been available for the examination of the heart for 100 years. It studies the function of the heart by examining the electrical potentials measured on the body surface. The interpretation of the causative electrical events within the myocardium constitutes the inverse problem. The electrical potentials recorded from body surface and displayed as ECG are formed by ionic currents across cell membranes, producing currents through the extracellular space between clusters of cardiac cells. These intercellular currents within the myocardium exhibit temporal and spatial patterns of activation and recovery, and are further affected by the properties of the volume conductor and the boundaries of the body surrounding the cardiac cells and the heart (Holland and Arnsdorf 1977). Any waveform on the surface ECG is generated by a voltage gradient within the heart (Hlaing et al. 2005).

ECG may be used as the basic diagnostic tool for a variety of cardiac conditions, the most important of which being myocardial infarction and myocardial ischemia. Chest pain is a common symptom with widely varying etiology. The most useful and widely applied tool in evaluating chest pain is the ECG. The main goal when recording and interpreting ECG in a patient with chest pain, is to identify cardiac ischemia and infarction. Of patients seeking medical help for chest pain approximately 20% have pain due to cardiac origin at the level of a general practitioner, and approximately 45% at the level of the emergency department (Erhardt et al. 2002).

Chest pain, unfortunately, is frequently absent, making diagnosis of MI difficult. At least one third of MIs go clinically undetected (Sigurdsson et al. 1995, Jonsdottir et al. 1998, Sheifer et al. 2001). The Framingham study data reveal that of ECG based incidence of MIs, 26% in men and 34% in women are clinically unrecognized (Kannel et al. 1990). The diagnosis of MI in this study, and most other studies, was based on the appearance of Q-waves in the 12-lead ECG. Thus, the incidence of unrecognized NQMIs is likely to be even higher (Sheifer et al. 2001). Yet, the prognosis after an unrecognized MI is as serious as after a recognized one (Sigurdsson et al. 1995, Kannel et al. 1990, Sheifer et al. 2001). In the Framingham study 10-year mortality in men was 58% and 49% following the detection of a clinically unrecognized MI and recognized MI, respectively, and in women 48% and 58%, respectively (Kannel et al. 1990). In the Reykjavik study the 10-year mortality figures were 51% and 38% for unrecognized and recognized MI, respectively (Sigurdsson et al. 1995). The incidence of unrecognized MI has also been estimated by serial follow-up ECG:s performed on a CAD free population at entry. Asymptomatic MI accounted for 22% of all nonfatal MIs. The 10-year prognosis after unrecognized MI was of similar magnitude than after a recognized one (risk ratio 1.7 vs. 1.5, respectively) (Yano and McLean 1989). In a more recent study the incidence rate of clinically unrecognized MI, detected by periodic ECGs, was 3.8 per 1000 person years as opposed to the incidence rate of clinically recognized MI of 5.0 per 1000 person years. The proportion of unrecognized MI was 33% in men and 55% in women (de Torbal et al. 2006).

In patients with unstable angina pectoris (UAP) 80-90% of the ischemic episodes are silent (Klootwijk et al. 1997) (Figure 1.). Yet, these painless episodes of ischemia are clinically important. In acute chest pain patients the ST-segment episodes during 12-lead

ECG monitoring are predictive of future myocardial infarction and myocardial death both at 5 and at 30 days (Klootwijk et al. 1998, Jenrberg et al. 1999).

These studies emphasize the importance of ECG as an epidemiologic tool, and in clinical use for diagnostics and in risk stratification, as well as in decision making for treatment strategies. The ECG, though being inexpensive, easily available, fast, and devoid of risk to the patient, is yet an unsatisfactory diagnostic tool with sensitivity and specificity for prior MI and acute myocardial ischemia less than desired.

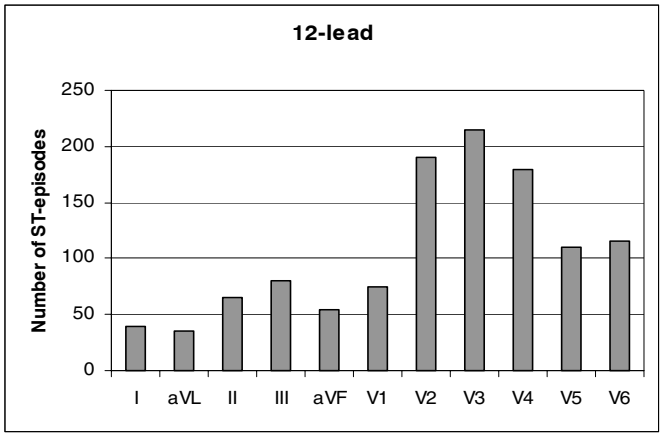

Figure 1 *Number of ischemic ST episodes per lead during continuous 48-hour 12-lead ECG monitoring in130 unstable angina pectoris patients (adapted from Klootwijk et al. 1997).*

2 REVIEW OF THE LITERATURE

2.1 Electrophysiology of depolarization

The myocardial cell resting membrane potential is 80-90 mV negative with respect to the outside of the cell. In the generation of the action potential (AP) an overshoot of +30 mV above the 0 membrane potential occurs resulting in a total of 120 mV action potential amplitude (Surawicz 1995a). This constitutes the depolarization of the myocardial cell. The QRS complex is the body surface manifestation of the rapid upstroke of the myocardial cellular AP (Geselowitz 1983). It is the display of the simultaneous noncancelled electrical potentials of a complex three-dimensional structure (Surawicz 1995b).

The ventricular depolarization begins in the subendocardial layers of the left side of the septum, spreads through to the apex, anterior left ventricular wall, reaching the epicardium and right ventricular septal surface. The endocardial activation is complete at approximately mid QRS. From the subendocardium of the basal regions the general spread of activation moves inferiorly, laterally and posteriorly (Surawicz 1995b).

2.2 Electrophysiology of repolarization

After the rapid upstroke of the cellular AP a prolonged plateau follows, maintained mainly by increase in Ca2+ conductance and inward Ca2+ current delaying repolarization (Antoni 1989, Fozzard and Makielski 1985). After the plateau the repolarization begins (Surawicz 1995a). This is the phase of restoration of the resting membrane potential. It is brought about by changes in the conductance of the cell membrane to K+ and outward current of positive ions (Antoni 1989, Fozzard and Makielski 1985).

The ECG manifestations of repolarization are the J wave, the T wave, and the U wave (Hlaing et al. 2005).

2.2.1 Transmural gradient of repolarization

A new cardiac cell type, the M cell, was discovered some 15 years ago (Sicouri and Antzelevitch 1991). It has unique electrophysiological properties, with prolonged AP and the propensity to further prolong the AP in response to various physiological and pharmacological stimuli, as compared to the epicardial and endocardial cells surrounding the M cell (Antzelevitch et al. 1999, Antzelevitch 2001). These different cell types, epicardial, endocardial, and the M cell, give rise to the physiological intramural heterogeneity of the repolarization, which exhibits, on the body surface, as the electrocardiographic T wave (Yan and Antzelevitch 1998). The first of these cell layers to repolarize is the epicardium. This creates a transmural voltage gradient directed from the

M cell layer toward the epicardium, which gives rise to the ascending limb of the T wave. The beginning of the T wave is the result of the divergence of the longer plateau phase of the M-cell AP from the shorter plateaus of the epi- and endocardial cells. The peak of the T wave coincides with full repolarization of the epicardium. The opposing gradient between the endocardium and the M cell layer limits the peak of the T wave and contributes to the descending limb of the T wave. The end of the T wave marks the full repolarization of the M cell layer (Antzelevitch 2001). The T-peak to T-end interval is an indicator of transmural dispersion of repolarization (Yan and Antzelevitch 1998). The electrocardiographic T wave is peaked when recorded along the transmural axis in a perfused wedge preparation of a canine heart and flattens out at a 90 degree angle to the transmural axis. This indicates that the electrocardiographic T wave is largely the result of the transmural voltage gradient (Yan and Antzelevitch 1998). Murine ECG does not usually exhibit T waves, but experimental adjustment of the ratio of the duration of epicardial and endocardial monophasic APs, to the ratio corresponding that of larger mammals, produces a T wave in murine ECG, as well (Liu et al. 2004).

2.2.2 Transventricular gradient of repolarization

The T wave concordance with the main deflection of the QRS is generally thought to result from opposite orientations of depolarization and repolarization (Franz et al. 1987). Transmembrane action potentials in the apex have been measured as shorter than in the base of the heart, thus having suggested producing an apico-basal gradient of repolarization (Noble and Cohen 1978). However, the apical potentials were actually recorded from the epicardium and the basal potentials at the endocardium reflecting, thus, difference between endocardium and epicardium rather than apex and base (Hlaing et al. 2005).

In a study by Franz et al. monophasic action potentials (MAP) were recorded at several endo- and epicardial sites in human hearts, in situ, simultaneously with surface ECG. They showed that activation time (AT), defined as the time from the earliest QRS deflection to the upstroke of MAP was regionally inversely correlated with action potential duration (APD) regardless of the recording site in the LV. Thus, with longer AT the APD shortens, synchronizing the repolarization times in the LV, regionally. The shortest endocardial ATs were recorded in the diaphragmatic and apicoseptal regions and the longest endocardial ATs in the anteroapical and posterolateral regions (Franz et al. 1987). The slope of the inverse correlation between AT and APD was -1.32, which would more than compensate for the longer ATs in the later activating regions of the left ventricle (LV) (Franz et al. 1987). Franz suggested this regional overcompensation being responsible for the normal concordance of the T wave with the QRS producing a repolarization wave of opposite direction to the depolarization wave, crediting transventricular gradient for the genesis of the T wave (Franz et al. 1991). However, regional endocardial repolarization times (RT), defined as the sum of AT and APD, were not significantly different between the different regions of the heart and produced no transventricular gradients (Figure 2.). In contrast, epicardial RTs were significantly shorter

than the endocardial ones, suggesting a transmural gradient of repolarization mainly responsible for the T wave. Endocardial ATs were shorter with longer APDs than in the epicardium, producing a transmural gradient of repolarization with an opposite direction to that of depolarization. The endocardial ATs fitted within the first third of the QRS deflection and the epicardial ATs within the first two thirds of the QRS (Franz et al. 1987).

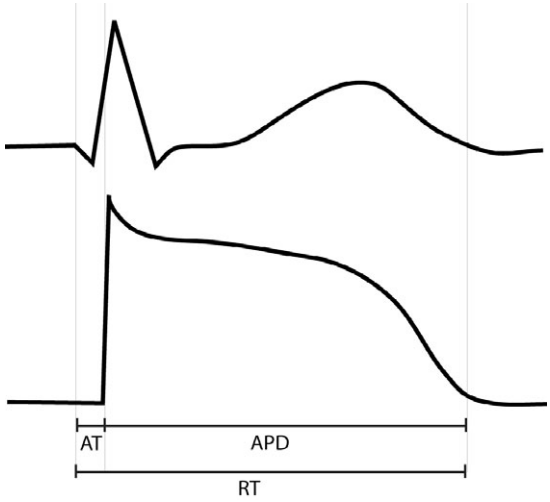

Figure 2 *AT=activation time, APD=action potential duration, RT=repolarization time, which is the sum of AT and APD (adapted from Franz et al. 1987).*

The endocardially recorded global depolarization sequence of the LV, in sinus rhythm, in the absence of conduction blocks, begins with the septum, proceeds eccentrically towards the free walls and apex and ends in the posterolateral basal areas (Yuan et al. 2001). The global repolarization sequence follows the activation sequence, with the end of the repolarization occurring in the same order. Despite that the activation time (AT), the time from the onset of the earliest depolarization of LV to local activation, was negatively correlated with monophasic AP duration, a regional overcompensation was not found in this study. The negative correlation of AT and MAP duration is insufficient to alter the sequence of repolarization from that of depolarization, and to be accountable for a transventricular gradient of repolarization in the direction concordant to the transventricular gradient of depolarization. The transventricular gradients do not, therefore, explain the concordance of the QRS and T waves in the normal heart. The repolarization sequence follows the depolarization sequence even in the presence of conduction blocks or ectopic activities inducing ST-T changes (Yuan et al. 2001).

A phenomenon called electrotonic modulation affects the duration of the action potentials by currents flowing between electrically well coupled tissues, retarding the repolarization of the areas activated earlier (Rosenbaum et al. 1982, Hoffman 1982). The electrotonic modulation is a slow, time-dependent process, as demonstrated by studies on

alteration of the activation sequence (Franz et al. 1991). The T-wave changes produced by changing the activation sequence by ectopic pacing take time to develop and even longer to disappear. Furthermore, with prolonged pacing the T wave reassumes concordance with the R wave, indicating tendency to synchronize the ventricular repolarization by the inverse correlation of AT and APD (Franz et al. 1991). In the case of left ventricular hypertrophy (LVH), the discordance of the R and the T waves is due to the lack of the inverse relationship of AT and APD (Franz et al. 1991).

In the canine heart no significant transventricular gradient of repolarization can be demonstrated (Yan and Antzelevitch1998). In humans both nondipolar (local) and dipolar (global) repolarization components probably contribute to the genesis of the T wave, with the relative contribution of each varying with varying clinical conditions (Hlaing et al. 2005).

The final manifestation of repolarization on the body surface ECG, the U wave, has been proposed to be an intrinsic part of repolarization process and attributable to small voltage differences between the ends of myocardial cell action potentials (Kors et al. 2005).

2.3 Ventricular gradient

The concept of ventricular gradient was introduced already 1934 by Wilson et al. The mean electrical axis of QRS gives the direction of the excitatory process over the ventricle, and the mean electrical axis of T gives the inverse of the direction of the recovery process. Were the excitation and recovery processes the same in time and mode, the sum of the QRS area (i.e. time integral) and the T area, the QRST area, would equal zero. The QRST area (i.e. time integral) measures the local variations in the excitatory-recovery process, and the mean QRST axis gives the direction of the line along which these local variations are the greatest (Wilson et al. 1934). The ventricular gradient is defined as the time integral of the lead voltage over the systolic electrical cardiac cycle, i.e. the QRSSTT integral (Geselowitz 1983). Should area under the myocardial cellular action potential be constant throughout the heart the ventricular gradient would disappear (Geselowitz 1983). As this is incorrect, a spatial variation in the form of action potential must exist. The ventricular gradient is the degree to which depolarization and repolarization do not cancel each other out in a certain body surface location (Flowers and Horan 1995). The ventricular gradient map, i.e. QRST integral map, provides the spatial estimation of dispersion of ventricular repolarization (Flowers and Horan 1995).

In thermally induced alteration in the recovery properties of canine hearts the QRST area (i.e. integral) change in ECG is related to the lesion severity (temperature) manifesting as increasing gradient contour lines in the body surface maps between affected and unaffected areas. The QRST area change showed a linear correlation with increasing temperature. When the temperature was kept constant and the size of the warmed area was increased, the density of the gradient contour lines on body surface maps remained the same with a larger altered region on body surface. The electrocardiographic QRST area (integral) change may thus be considered an index of lesion severity and the

body surface area affected an index of the lesion size (Burgess et al. 1978). QRST area (integral) also appeared independent of the activation sequence in contrast to the QRS and ST-T areas, in both body surface distribution and quantitatively. This indicates that the QRST area (integral) reflects intrinsic ventricular recovery properties (Lux et al. 1980).

2.4 Clinical applications of the depolarization, the repolarization, and the ventricular gradients

The ventricular gradient or its equivalents have value as prognostic risk factors in post MI patients. Several parameters or features other than QRSSTT integral describe approximately the same phenomenon: spatial divergence of the main directions of the depolarization and repolarization wavefronts. The numerous ways of describing this phenomenon include mirror image reversal, total cosine between R and T (TCRT), QRS-T axis, among others. Several problems still remain with some of these features. The mirror image reversal (Maynard et al. 2003) may be observed visually, as body surface maps, but this kind of observation is difficult to quantify and to approach statistically. The reduction of the mirror image reversal into a planar vector angle between the minima and maxima of the maps loses a lot of information otherwise obtainable from the body surface maps. Furthermore, the acquiring of the body surface maps is arduous and not practical in acute or monitoring situations.

The TCRT, which describes the 3-dimensional angular difference between the spatial QRS and T wave loops derived from the 12-lead ECG, is a unitless scalar measure of the angle between the depolarization and repolarization vectors. It is considered to reflect increased repolarization heterogeneity (Batchvarov et al. 2004). This parameter holds much promise and has been shown, in several studies, to be of prognostic value (Batcvarov et al. 2004, Malik et al. 2004, Zabel et al. 2000). This variable can be approached as a continuous variable between –1 and 1. High positive values of TCRT indicate a small angle between the vectors up to a point where the vectors are parallel, when the TCRT value is 1. From thereon the angle starts to increase again with decreasing TCRT values up to a point when the vectors are at a 180-degree angle to each other, when the TCRT is –1 (Batcvarov et al. 2004).

Studies have shown associations between conduction disturbances (LBBB) and greater divergence of the wavefronts as compared to the parallelism of the wavefronts in the normal heart (Maynard et al. 2003, Zabel et al. 2000). More importantly, studies have shown the association of this divergence with adverse cardiac events, mainly arrhythmias, and death (Zabel et al. 2000, Malik et al. 2004). The association remains even in the presence of conduction disturbances (Zabel et al. 2000). TRCT distinguishes between patients with hypertrophic cardiomyopathy and normal subjects, with TCRT being negative in patients with hypertrophic cardiomyopathy and positive in normal subjects (Acar et al. 1999).

The spatial angle (QRS-T angle) between the depolarization and repolarization orientations can also be projected on a frontal plane and categorize the planar angles as normal, borderline, or abnormal (de Torbal et al. 2004). This categorical variable holds

similar diagnostic and prognostic information to the TRCT. Spatial QRS-T angle, computed from reconstructed vectorcardiographic leads, is a strong and independent predictor of cardiac mortality, sudden death, and total mortality in general population of over 55 years of age (Kardys et al. 2003). The spatial QRS-T angle exceeded the classical cardiovascular and ECG predictors as a prognostic factor. Interestingly, however, it was unable to predict non-fatal cardiac events. The authors' suggestion is that abnormal QRS-T angle is a sign of myocardial damage leading to propensity for ventricular rhythm disturbances resulting in fatal events, and to a lesser extent in non-fatal events. The QRS-T angle is an independent predictor of long-term (6 years) mortality in patients with symptoms suggestive of acute cardiac pathology, whereas the frontal T-axis is additionally an independent predictor of acute cardiac pathology and short-term mortality (de Torbal et al. 2004). For the QRS-T angle, either, conduction abnormalities had no effect on the prognostic value of the variable. The problem with this variable is its categorical nature, which makes correlation with continuous variables difficult. In addition, it reduces the spatial information content of the recordings onto a plane.

The spatial QRS-T angle is reduced after successful thrombolysis in acute MI, whereas an unsuccessful thrombolysis does not affect the parameter. However, the QRS-T angle is inferior in estimating artery patency after thrombolysis as compared to the recommended ST-segment resolution (Dilaveris et al. 2005). The spatial QRS-T angle and spatial T amplitude do not differentiate between recent (5-10 days) and old (>6 months) MI, but distinguish them from healthy controls (Dilaveris et al. 2001).

Minor T-wave abnormalities (Minnesota Code 5.3 or 5.4) have independent long-term (6 years and 18.5 years) prognostic value for CHD and cardiovascular mortality in a cohort of men at high risk but free of CHD at entry (Prineas et al. 2002). Spatial T-axis deviation has independent prognostic value, in a cohort of elderly (≥65 years) men and women free of CHD at entry, with regard to CHD death (adjusted hazard ratio 2.0), incident CHD (adjusted hazard ratio 1.6), and all-cause mortality (adjusted hazard ratio 1.5). With increasing T-axis deviation, several cardiovascular risk factors, including the internal carotid intima-media thickness, increased. The hazard ratios were calculated after adjusting for other CHD risk factors, including other ECG abnormalities, of which only QT prolongation was associated with increased risk. Despite pronounced T-axis orientation differences, the QRS axis was fairly unchanged. The authors conclude that the T-axis deviation is a subclinical sign of cardiac abnormality and results from action potential duration change in any ventricular region (Rautaharju et al. 2001). In a cohort of men and women of ≥55 years of age the T-axis deviation was associated with several cardiovascular risk factors. Yet, after adjustment for these factors and several ECG variables (QTc interval, QT dispersion, ST depression, T-wave inversion, MI by ECG, LVH by ECG) the risk associated with abnormal T-axis was higher than for any other risk factor or ECG indicator (hazard ratio 2.8 for cardiac death), suggesting that T-axis carries information beyond other ECG variables, and is a marker for subclinical myocardial damage. The authors recommend its usage in clinical practice and in screening programs (Kors et al. 1998).

An initially promising measure of repolarization abnormality, QT dispersion, thought of describing spatial dispersion of repolarization, appears to be a manifestation of different

projections of a common T-wave vector onto the surface ECG, instead of describing variation in AP duration at locations adjacent to recording leads (Kors et al. 1999, Malik et al. 2000). Another measure of repolarization heterogeneity, T-wave residuum (TWR), has shown prognostic power for mortality in population with cardiovascular disease (Zabel et al. 2002).

In experimental myocardial infarction of 12 canine hearts a measure of electrical field dipolarity (equivalent generator ratio) investigated by BSPM, expressed as percentage, during QRS, ST, and QRST waveforms was studied. The dipolarity content was high (over 96%) before MI during all of these periods. One week post MI the dipolar content was reduced during the QRS (62% in posterior MI and 91% in anterior MI) but not during ST and QRST waves (Claydon et al. 1991).

2.5 Electrophysiology of the ischemic myocardial tissue

The ST-segment shift in the acutely ischemic myocardial cell is considered to result from the summation of the baseline (TQ-segment) shift and actual ST segment displacement, (Holland and Arnsdorf 1977, Holland and Brooks 1977) (Figure 3.). During the electrical diastole the ischemic cells exhibit less negative resting potential than normal cells, producing an injury current from the ischemic region to normal myocardium causing a shift of the TQ segment to the opposite direction of the facing electrode. During the plateau phase of the action potential, which normally is isoelectric in the ECG, the ischemic cells show incomplete depolarization or alternatively a shortened plateau, producing an injury current into reversed direction. This results in the ST segment shift in the direction of the facing electrode (Holland and Arnsdorf 1977, Holland and Brooks 1977). Evidence from open-chest dog studies show the TQ-segment shift to be the dominant change with true ST-segment shifts to be of a lesser magnitude and variable in expression showing both elevation and depression (Vincent et al. 1977). In the ischemic cardiac tissue the extracellular K+ concentration is increased either due to the increased permeability of the cell membrane to K+, resulting in the efflux of K+ or to the inhibition of the sodium-potassium adenosine triphosphatase (Na+- K+ ATPase) pump and its transport of K+ into the cell. The increased K+ concentration brings about the lowering of the resting membrane potential and reduction of action potential duration (Holland and Arnsdorf 1977, Holland and Brooks 1977). The efflux from the ischemic cell of K+, without influx of Na+, is accompanied by loss of anions from the cell. Metabolic generation of lactic acid leads to a transfer of protons to the proteins mainly responsible for the negative charge of the resting cell. This decreases the anions inside the cell and increases the anions that can leave the cell (Fozzard and Makielski 1985).

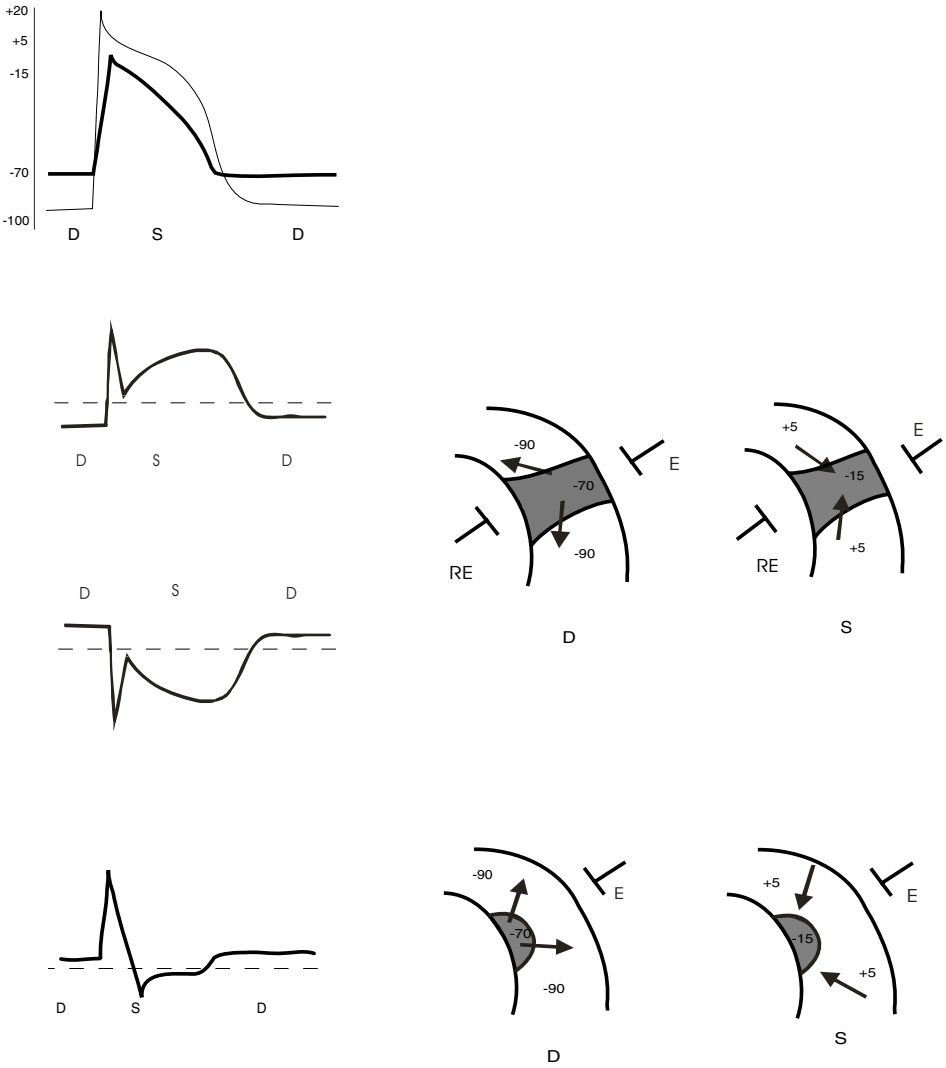

Figure 3 *In the left panel the upper graph presents the action potential (AP) of the normal myocardial cell (thin line) and the ischemic myocardial cell (thick line). The following graphs present the corresponding ECGs, with the isoelectric line (broken line), with transmural ischemia viewed from the facing electrode (E), transmural ischemia viewed from the reciprocal electrode (RE), and subendocardial ischemia viewed from the facing electrode, respectively. The images on the top right present injury current in transmural ischemia in diastole (D) and systole (S) and the images on the bottom right the respective injury currents in subendocardial ischemia viewed from the facing electrode.The shaded area represents the ischemic myocardium.*

In the ischemic myocardial cell decrease in resting membrane potential occurs during the first minute of ischemia followed by shortening of action potential duration, which together result in ST-segment displacement (Kleber et al. 1978). MAPs of the ischemic myocardium show an increase in AT caused by retarding of the conduction velocity (Franz et al. 1991). ST-segment elevation is the result of ischemia in the leads recording over the ischemic myocardial area. This primary ST-segment elevation may always be seen as reciprocal ST-segment depression on the opposing body surface. Registered ST-segment depression may, alternatively, be primary and reflect subendocardial ischemia (Mirvis 1988). An acute obstruction to coronary blood flow results in transmural, supply-type ischemia producing ST-segment elevation in the facing electrode and ST-segment depression in the reciprocal electrode, whereas incomplete coronary occlusion with diminished bloof flow results in demand-type, subendocardial ischemia, producing ST-segment depression in the facing electrode (Figure 3.). Whether the ECG alterations are local or reciprocal may be determined by activation-recovery interval, which is altered by local injury but remains unaltered over the reciprocal region, despite other reciprocal ECG alterations such as QRS, ST-T, and QRST areas. The activation-recovery interval is defined as the interval between the times of the minimum derivative of the QRS complex and the maximum derivative of the T wave (Ikeno et al. 1995).

The first report of ECG alterations during myocardial ischemia demonstrated the ST-segment elevation as characteristic to ischemia (Pardee 1920). ST-T changes are generally regarded as ECG signs of myocardial ischaemia and changes in the QRS pattern as myocardial necrosis (van De Werf et al. 2003). However, early in the course of acute MI the ECG is often equivocal and may never show ST elevation or new Q waves (Van de Werf et al. 2003). Current techniques with sensitive and specific biomarkers and imaging techniques can identify myocardial necrosis of <1.0g (Thygesen and Alpert 2000). During ischemia the cell death begins to develop after 15 minutes, and complete necrosis of myocardial cells in the area at risk takes 4-6 hours, or longer (Thygesen and Alpert 2000). The electrocardiographic Q waves develop within 6 to 14 hours after the onset of symptomatic myocardial ischemia (Essen et al. 1980). The resolution of the ST segment changes is considered a sign of withdrawing of ischemia (Thygesen and Alpert 2000). During balloon inflation-induced acute myocardial ischemia the electrocardiographic changes, ST-segment elevation and reciprocal ST-segment depression, appear within 19±12 seconds and resolve within 20±9 seconds of deflation. The echocardiographic wall motion abnormalities are evident prior to the ECG changes, within 15±5 seconds after inflation, and disappear within 13±3 seconds of deflation (Griffin et al. 1987). In a similar study the echocardiographic hypokinesia began 19±8 seconds, and started to normalize within 17±8 seconds (Hauser et al. 1985).

2.6 The standard 12-lead ECG in diagnosing myocardial infarction

2.6.1 Prior MI

Conventionally, the ECG diagnosis of prior MI is based on the initial QRS abnormalities. This applies to a number of coding systems as well as clinical decision making. In a recent consensus conference (Thygesen and Alpert 2000) the ECG criteria for established MI was defined as the presence of a Q-wave with duration of ≥30 ms in V1-V3, or abnormal Q wave in at least two contiguous leads at lest 1 mm in depth. Changes in the QRS pattern are considered signs of myocardial necrosis (Figure 4.). According to the consensus conference Q waves of shorter duration may also indicate myocardial necrosis, but require more research as does the depth of the Q wave. Normal ECG does not exclude myocardial necrosis, especially when the necrosis is of microinfarction size and detectable only with the sensitive biomarkes (Thygesen and Alpert 2000).

In comparison of nine electrocardiographic computer programs' and eight cardiologists' ability to interpret ECGs with seven different clinical diagnoses, and normals, the diagnostic sensitivity for anterior MI was 77% vs. 85%, and for inferior MI 59% vs. 72%, and for combined MI 59% vs. 68%, respectively, with equal specificities (Willems et al. 1991).

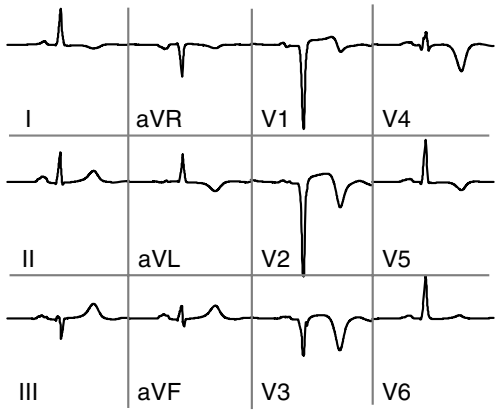

Figure 4 *A 12-lead ECG with a Q-wave myocardial infarction.*

2.6.2 Coding systems for myocardial infarction

2.6.2.1 The Minnesota code

The Minnesota code is a complex, descriptive code including various electrocardiographic conditions, such as ventricular conduction defects, arrhytmias etc. It is widely used in epidemiological practice. For MI there are different categories of descriptions based on Q-wave amplitudes and durations or Q/R amplitude ratios in different combinations of leads for different MI locations. In addition to the Q and QS patterns, the code includes descriptions for ST and T wave abnormalities, but sets no explicit diagnoses (Macfarlane 1989a,b). The Minnesota Q-QS codes of 1.1, 1.2, and 1.3 refer to definite, probable, and possible Q-wave MI, respectively (Pahlm et al. 1998). In a study with MI verified at autopsy the sensitivities of Minnesota codes 1.1, 1.1-2, and 1.1-3 were 33%, 52%, and 62% at a specificity levels of 98%, 94%, and 88%, respectively. The Q-QS abnormalities occurred more frequently in recent than old MIs, in anteroseptal than posterior or lateral MIs, and in transmural than in subendocardial lesions. However, a substantial proportion of subendocardial MIs showed codable Q waves. In this study 50% of old MIs and 40% of all MIs exhibited no diagnostic Q waves (Uusitupa et al. 1983).

2.6.2.2 The Selvester score

The Selvester QRS scoring system was designed to estimate the MI size from the 12-lead ECG. It was developed using a computer simulation of the heart activation sequence. It consists of 54 criteria, including R and Q wave amplitudes, durations, and the ratios of R-to-Q and R-to-S amplitudes; with a point score for each. The maximum point score is 32 points, each representing 3% of the LV (Selvester et al. 1985). The Selvester score is proportional to the severity of wall-motion abnormalities determined by radionuclide scanning and inversely correlated with LVEF (Palmeri et al. 1982). In comparison with CE-CMR in patients with a prior single anterior MI the Selvester score showed a correlation of r=0.40 with MI size (Engblom et al. 2003). In the detection of prior MI a subset of 3 criteria with an automated computer application has shown a sensitivity of 77% with a specificity of 86% (Pahlm et al. 1991). The complete automated Sylvester score achieved sensitivity of 67%, 41%, 32%, and 72% at a 95% specificity level for anterior, inferior, posterolateral, and multiple MIs, respectively (Haisty et al. 1992).

2.6.2.3 The Cardiac Infarction Injury score

Designed for epidemiological studies and clinical trials the Cardiac Infarction Injury Score (CIIS) detects prior MI with sensitivities of 85% and 71% at specificity levels of 95% and 99%, respectively. It is intended for visual coding containing a checklist of 12 items measured from the 12-lead ECG with continuous and discrete features each having a

weight factor for the final contribution to the total score. A considerable number of these features (5 of 12) are based on T-wave amplitude. The CIIS performs best on MIs 1 week to 1 months of age, but retains a sensitivity of 80% at a specificity level of 98%. The code may be used also for serial comparisons of ECGs. Graded severity levels may be used for populations of different prevalence levels of MI. Yet, the use of the code is relatively time consuming: a technician can code approximately 20 ECGs an hour (Rautaharju et al. 1981).

2.6.2.4 The Washington code

The Washington code, published 1982, applies the vectorcardiographic X, Y, and Z leads in setting the diagnosis of MI. The criteria employ simple amplitude and duration criteria, in addition to amplitude ratio criteria. Two levels of criteria may be used depending on the desired sensitivity. Different criteria are set for men and women, black and white. The Washington code is more sensitive than the Minnesota code in diagnosing MI (Macfarlane 1989a). The beauty of this code is its simplicity: the criteria are based on Q/R amplitude ratio and a diagnostic limit is defined for each lead, X, Y, and Z, in each of the patient groups, with two optional sensitivity levels. The code has shown sensitivities of 71% and 75% at specificity levels of 93% and 87%, respectively (white patients), exceeding in performance the Minnesota code. A computer program for the Washington code has also been developed (Macfarlane 1989a,b, Pipberger 1982).

2.6.2.5 The Punsar code

The Punsar code was designed to diagnose ischemic heart disease by ST-segment alterations. It classifies ST-segment changes into three main categories according to the degree of ST-segment depression and quality of the ST depression, horizontal, downward sloping, slowly ascending or rapidly ascending. The first of the categories, comprising horizontal and downward sloping ST depression is labeled ischemic (Macfarlane 1989a,b).

2.6.2.6 The Novacode

The Novacode, designed for serial comparisons of ECGs, is based on the Minnesota code. It accepts any negative initial deflection as a Q wave and considers the amplitude and duration of the Q wave as a continuous parameter (Pahlm et al. 1998).
In a study comparing the efficacies of 4 coding systems in estimating MI size verified at autopsy, the Selvester score was superior (r=0.70) to the Minnesota code (r=0.51), Novacode (r=0.50), and the CIIS (r=0.43). All the codes performed best with MIs in the anterior location. The performance was poor for all the codes with MIs in multiple locations (r range 0.18-0.44) (Pahlm et al. 1998).

Based on the Selvester QRS coding system a computerized algorithm (Cardiovise 2.0) has been developed to detect, size, and localize prior MI. In addition to the QRS criteria, it applies T-wave criteria, and has been designed to detect also NQMI. The Cardiovise 2.0 has been compared with the diagnostic ability of experienced cardiologists and primary care physicians, as well as two commercially available EGC diagnostic algorithms. The Cardiovise reached the same sensitivity as the cardiologists and primary care physicians (52%), higher than the two commercial algorithms (28% and 24%). The specificity of the Cardiovise 2.0 (97%) was comparable to that of the cardiologists' (93%), and the commercial algorithms' (99% and 96%), and higher than that of the primary care physicians' (72%) (Wagner et al. 2002). The Cardiovise was further improved to versions 2.5 (Andersen et al. 2001) and 3.0, the latter reaching sensitivity of 69% and specificity of 96% in the detection of prior MI. It also contained an algorithm for the detection of ST-elevation AMI (STEMI) and non-ST-elevation AMI (NSTEMI) reaching sensitivities of 83% and 52%, respectively and specificity of 94% (Andersen et al. 2002).
A study by Warner et al. has indicated that in addition to depolarization abnormalities, repolarization alterations, especially in the T wave amplitude, may be of value in diagnosing prior MI and enhance the diagnostic performance of the QRS criteria (Warner et al. 1988).

Techniques used in BSPM have also been applied to the 12-lead ECG, analyzing non-conventional parameters, outside the initial QRS, and applying discriminant analysis (Kornreich et al. 1992). A combination of 7 non-conventional features yielded a sensitivity of 89% with a specificity of 92% for the detection of prior QMI. In the acute situation the same combination of features achieved a correct classification of 72% in NQMI and 85% in QMI.

2.6.3 Acute MI

The currently valid ECG criteria for acute evolving MI are ST-segment elevation in at least two contiguous leads, at the J point, of ≥0.2 mV in V1-V3, and ≥0.1mV in other leads (Figure 5.). Alternatively, equivocal criteria of ST segment depression or T-wave abnormalities only in at least two contiguous leads (Thygesen and Alpert 2000). These criteria are set by a consensus committee and are based on clinical experiment and studies with varying criteria for acute MI. In a study of over 1000 chest pain patients the optimal threshold for the ST-elevation in detecting AMI proved to be ≥0.1 mV in inferior/lateral leads or ≥0.2 mV in anteroseptal leads (Menown et al. 2000b).

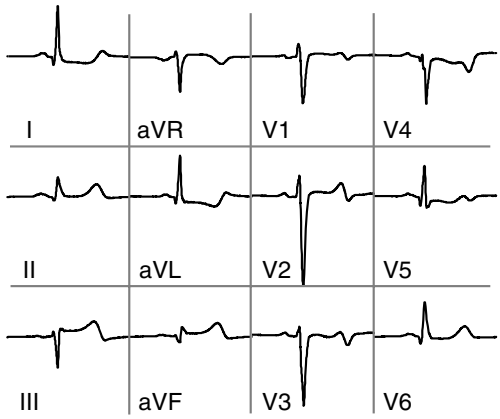

Figure 5 *A 12-lead ECG with evolving myocardial infarction.*

In the setting of acute chest pain, the standard 12-lead ECG only has a sensitivity of less than 60% for MI (Carley et al. 2003). Yet it remains the most important tool for patient triage in the acute situation, and also for the choice of treatment. Several reasons account for the failure of the 12-lead ECG: the location of the ischemia is unapproachable with the standard lead placement (Carley et al. 2003), presence of LBBB, prior MI or LVH with altered baseline ECG, etc. Yet, LBBB, in the setting of acute MI, carries a higher risk of death, whatever its onset. New onset LBBB is a negative prognostic factor in the face of acute ischaemia, indicating ischaemic conduction damage, whereas old LBBB is associated with worse pre-infarction characteristics and thus carries worse prognosis (Wong et al. 2006).

As the 12-lead ECG criteria for evolving myocardial infarction (Thygesen and Alpert 2000) has deficient sensitivity, attempts have been made for improving the performance by broadening the criteria in the 12-lead ECG. These attempts have lead only to modestly improved sensitivity, with the cost of loss of specificity (Self et al. 2006). The precordial 6-lead system was popularized during the 1930s and 1940s. Research on other useful chest recording locations, at that time, failed to reach consensus, and the 6 chest leads became the standard (Self et al. 2006).

The ST-segment elevation in patients with evolving acute MI is of low sensitivity (53-55%), but relatively high specificity (86-95%). Moreover, it is transient, even in the absence of treatment. Adams has stated that the ECG criteria for thrombolytic treatment are too insensitive missing a substantial proportion of patients who might benefit from thrombolysis. He suggested thrombolytic therapy administered in all patients presenting very early with symptoms suggestive of AMI and an abnormal ECG (Adams et al. 1993). Approximately 5% of patients with suspected ACS and normal ECGs, who were discharged from the emergency department (ED), were ultimately diagnosed with AMI or UAP (Bertrand 2002). The inappropriate discharge due to normal ECG affects more often women than men (Erhardt et al. 2002).

The sensitivity of the initial 12-lead ECG in diagnosing AMI is 13-69% (Speake and Polly 2001) (Table 1.).

Table 1. *The sensitivity of the initial 12-lead ECG in diagnosing acute myocardial infarction in several studies.*

	Patients	Study type	Sensitivity of initial ECG %
McGuinness BJ et al, 1976, Scotland	898 patients admitted to CCU, 400 with AMI	Prospective	51
Starck M, Vacek JL, 1987, USA	221 ED chest-pain patients, 39 with AMI	Prospective	62
Sharkey SW et al, 1988, USA	34 patients admitted to CCU, 34 with AMI	Prospective	61
Fesmire F et al, 1989, USA	440 ED chest pain patients, 100 with AMI	Prospective	47
Rouan G et al, 1989, USA	918 ED chest pain patients, 811 with AMI	Prospective	13
Gibler B et al, 1992, USA	616 ED chest pain patients, 108 with AMI	Prospective	36
Young P, Green T, 1993, USA	222 ED chest pain patients, 43 with AMI	Retrospective	28
Zalenski R et al, 1993, USA	149 ED chest pain patients, 34 with AMI	Prospective	47
Fesmire F, 1998, USA	1000 ED chest pain patients, 204 with AMI	Prospective	55
Kudenchuk PJ et al, 1998, USA	3027 ED chest pain patients, 1149 with AMI	Prospective	69

AMI=acute myocardial infarction, CCU=coronary care unit, ED=emergency department.

Non-specific ECG changes, such as ST-depression and T-wave inversion in the setting of acute chest pain may also indicate evolving AMI (Thygesen and Alpert 2000). ST-segment depression and even T-wave inversion indicate worse prognosis (increased long term mortality) in comparison with normal ECG. Non-specific ST-changes are a more important predictor of mortality than elevation of TnT. When these two independent predictors are combined, three groups of different levels of risk are formed: low (normal TnT, no ST-segment depression), intermediate (elevated TnT or ST-segment depression), and high (elevated TnT and ST-segment depression). The non-specific ECG changes were an even more important prognostic sign in women than in men (Jernberg et al. 2002). The risk for subsequent cardiac events in patients estimated on the basis of admission ECG is in decreasing order: ST-segment elevation, ST-segment depression, T-wave inversion, and normal ECG (Bertrand et al. 2002, Erhardt et al. 2002).

Computer protocols have been developed to aid or replace clinicians in the decision making in acute chest pain. A computer protocol to detect acute myocardial infarction was prospectively tested on almost 5000 chest-pain patients. This protocol reached a sensitivity of 88.0% and a specificity of 74%, as opposed to sensitivity 87.8% and specificity of 71% achieved by a physician, thus being as effective as and less costly than the clinicians' evaluation with regard to patient triage (Goldman et al. 1988).

In the pre-hospital setting hospital based algorithms are unsuitable for patient triage and diagnosis prediction in chest-pain patients. The most important predictor of cardiac pathology is an abnormal ECG (Grijseels et al. 1995).

In acute coronary syndrome patients with successful angioplasty, in whom the ST-segment completely resolves at 60 minutes, the extent of myocardial damage is smaller and prognosis better as compared to those with partial or no resolution (Van't Hof et al. 1997). ST-monitoring pre-, during, and post-angioplasty of acute STEMI patients has shown that lack of resolution of or increase of ST elevation indicates worse prognosis (Terkelsen et al. 2006). Yet, 41% of the patients with spontaneous resolution of the ST segment had insufficient reperfusion at angiography before PCI. Based on this study continuous ST-segment ECG monitoring pre- and during PTCA and an assessment of ST-resolution 30 min after the procedure is recommended (Aude and Mehta 2006). The reperfusion syndrome is defined as additional ST-segment elevation upon reperfusion. This electrocardiographic phenomenon is probably a marker of microcirculatory reperfusion injury and predicts larger MI size and more severely impaired LV function as compared to patients without reperfusion syndrome (Feldman et al. 2000).

Nearly 2/3 of ischemic episodes in unstable coronary artery disease are silent. Patients with transient, asymptomatic ST-segment changes have increased risk of cardiac events (Bertrand et al. 2002). One reason for electrocardiographically silent ischemia in the 12-lead ECG is the site of the lesion and the complex relationship of the heart and the torso, as demonstrated by torso tank experiments with a perfused canine heart (MacLeod et al. 1998).

2.6.4 Q wave and non-Q-wave myocardial infarction

The designation of MI as QMI or NQMI is purely descriptive, reclining to the prespecified changes in the 12-lead ECG. Q wave may, thus, occur also in a normal heart and be absent in a heart with a myocardial scar. The presence of a Q wave is related to the size of MI (Mirvis 1985). In a contrast enhancement cardiac magnetic resonance imaging (CE-CMR) study in patients with previous MI, the Q wave was found to predict the size of MI and LV function, rather than the extent of transmurality of MI. Areas under receiver operating characteristics curve (AUC) for anterior MI and inferior MI were 90% and 77% for the prediction of Q-waves by the MI size. No relationship in the lateral territory was found. CE-CMR has also shown that MIs are of a complex structure and division into transmural vs. subendocardial MIs is over-simplistic (Moon et al. 2004) (Figure 6.). Also BSPM studies have indicated that the injury in NQMI is smaller than in QMI and that NQMI is a heterogenous entity, both in electrocardiographic terms and ventriculographic patterns. A

part of NQMIs are, in fact, QMIs revealed by BSPM recordings outside of the standard 12 leads (Montague et al. 1986). Patients with NQMI have less necrosis, fewer segments with impaired LV wall motion, higher LVEF, and fewer persistent 201Tl defects than patients with QMI. However, the cardiac long term mortality is similar in NQMI and QMI patients. This might be explained by higher reinfarction rate and a higher rate of ACS requiring hospitalization and revascularization procedures in patients with NQMI. Majority of the reinfarctions in NQMI patients involve the same area as in the original MI (Gibson et al. 1986). Patients with NQMI have lower in-hospital mortality but a similar long-term (8 years) survival as compared to patients with QMI (Goldberg et al. 1987). NQMI patients have shown lower short term (6 months) mortality, but higher long term mortality (3 years) than QMI patients (Krone et al. 1983).

Even though QMIs are generally referred to as transmural and NQMIs as non-transmural, studies using CE-CMR as a reference for the determination of transmurality have not been able to show that the 12-lead ECG can distinguish between transmural and non-transmural MIs (Sievers et al. 2004, Moon et al. 2004). QMI is, however, a predictor of the size of MI (Moon et al. 2004, Kaandorp et al. 2005). In accordance with this, the QRS area sum, in both 12-lead ECG and optimal BSPM leads, correlates well with LV mass in LVH patients (Oikarinen et al. 2004). Ischemic and viable myocardium, determined by positron emission tomography, after NQMI is more common than after QMI (Yang et al. 2004). A quantitative difference with a smaller MI size in NQMI than QMI, rather than them being two distinct clinical entities, is indicated also by the lower frequency of echocardiographic wall motion abnormalities and higher ejection fraction in the NQMI patients, as well as quantitative rather than qualitative differences in BSPM maps (Kornreich et al.1991).

When CE-CMR was used as reference, endocardial unipolar potentials acquired by electromechanical mapping in post MI patients were reduced in segments with subendocardial (6.8±2.9 mV) and transmural (4.6±1.9 mV) injury, as compared to normal segments (11.6±4.5mV). The voltage difference between the subendocardial and transmural MI, however, failed to reach significance (Perin et al. 2002). Thus, also by endocardial mapping, transmural and subendocardial MIs are indistinguishable.

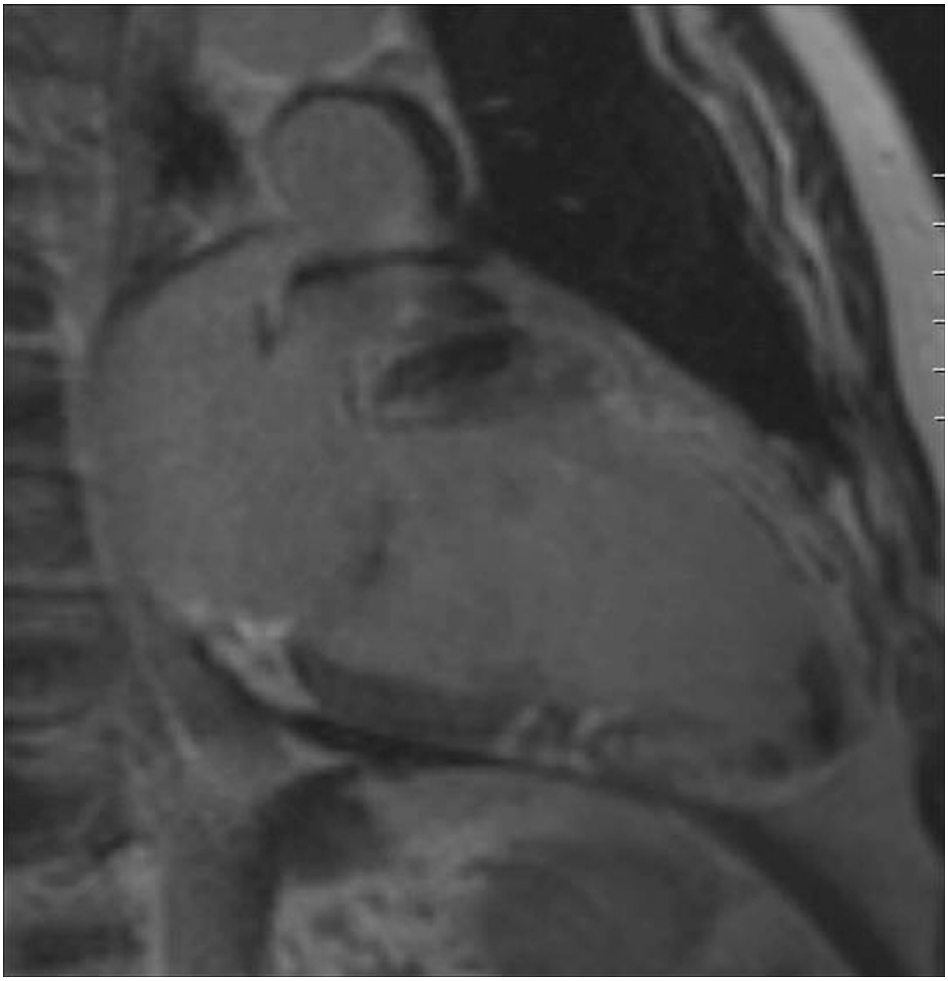

Figure 6 *Contrast enhancement magnetic resonance image of an extensive, myocardial infarction with heterogeneous contrast enhancement (bright areas) with respect to the myocardial thickness, demonstrating the variability in the transmurality of the myocardial scar.*

2.6.5 ST-segment elevation and ST-segment depression myocardial ischemia

Acute coronary syndromes have a common underlying pathophysiology of atherosclerotic plaque erosion or rupture with superimposed thrombosis. Unstable angina and evolving myocardial infarction are the ensuing clinical presentations of this process (Bertrand et al. 2002). In the European Heart Survey on ACS 42% of patients presented with STEMI, 51% with NSTEMI or normal ECG, in 7% the ECG was undetermined (BBB, pacemaker) (Battler 2002).

For patients with symptoms suggestive of acute ischemia and persistent ST elevation, indicating transmural ischemia by coronary occlusion, early PCI or fibrinolytic treatment should be performed without delay, unless contraindications are present (Van de Werf et al. 2003). For chest-pain patients with persistent or transient ST-segment depression, T-wave inversion, flat T-waves, pseudo-normalization of T waves, non-specific ECG changes, or even normal ECG at presentation fibrinolytic therapy is not recommended. These patients should be observed with repeated ECG:s and ST-segment monitoring, and repeated biochemical marker measurements. The goal is to alleviate ischemia with medical treatment and to estimate the patient's risk: high-risk or low-risk. For high-risk patients GPIIb/IIIa receptor inhibitors and coronary angiography within 48 hours, and for low-risk patients a stress test are recommended (Bertrand et al. 2002).

Yet the studies on ST-elevation and ST-depression MI are equivocal. A placebo versus recombinant tissue-type plasminogen activator thrombolysis treatment late in the acute MI were compared in a large study (LATE; the Late Assessment of Thrombolytic Efficacy) comprising 5711 patients with suspected acute coronary syndrome. At hospital discharge the QMI versus NQMI-status were determined. NQMI patients had, at 1 year, similar reinfarction rate but lower mortality as compared to QMI patients, irrespective of treatment assignment. Patients with ST-elevation MI had no benefit from rt-PA as compared to placebo at 1 year in terms of mortality, whereas patients presenting with ST-depression MI benefited from rt-PA treatment in terms of mortality at 1 year. However, a subgroup of ST-elevation MI patients receiving rt-PA within 3 h of hospital admission had lower mortality as compared to those treated with rt-PA later. The authors conclude that NQMI is a heterogenous entity and that late thrombolysis may benefit patients presenting with ST-depression (Langer et al. 1996). Patients with ST-elevation MI, treated with thrombolysis, subsequently evolving into NQMI (21% of patients) showed better 30- day and 1-year prognosis than patients developing QMI, but needed angioplasty more often than QMI patients (Barbagelata et al. 997). In GUSTO-IIb study comprising over 12 000 patients with acute coronary syndrome the 30-day mortality or reinfarction rate were as high as 11% in patients presenting with ST-segment depression, 9% in patients with ST-segment elevation, and 12% in patients with both ST-segment elevation and depression (Savonitto et al. 1999). ACS patients with ST depression only have a high mortality of 16-19% not reduced by thrombolytic therapy (GISSI 1986, ISIS-2 1988). Patients presenting with initial ST depression and symptoms suggestive of ACS have a 1-year mortality of 31% (Lee et al. 1993).

A study comparing thrombolysis vs. placebo and early invasive versus conservative strategy in patients considered of having acute NMQI (transient ST elevation or ST depression or T-wave inversion and ACS symptoms) showed no benefit from thrombolysis, whereas early invasive strategy benefited the patients in terms of reduced hospitalization (TIMI IIIB 1994).

In some patients registered ST-segment depression may be a reflection of a reciprocal ST-segment elevation indicating AMI recorded on the opposing body surface (Mirvis 1988). In these patients thrombolysis might be beneficial (Braunwald and Cannon 1996).

ST depression in 12-lead ECG in patients with symptoms suggestive of acute MI is a highly specific marker of MI and is related to poor prognosis (Lee et al. 1993). Even when MI was acutely excluded, the ST depression indicated high (19%) 1-year mortality. Moreover, the degree of ST depression was related to mortality. In this study a substantial proportion of patients received thrombolytic therapy, despite lack of ST elevation criteria. Those patients tended to have lower mortality, but the difference between mortalities was not significant. The degree of the ST depression was more important marker of MI than the number of leads carrying the abnormality, indicating that the choice of the right parameter and selection of appropriate threshold value are more important than the abundance of information gained. The authors conclude that a severe ST depression might be an indication for thrombolysis. However, some patients with severe ST depression may have unstable angina and it would be important to be able to distinguish these patients quickly from those who have evolving MI. ST depression in the absence of ST elevation can be the only ECG abnormality in transmural MI, confirmed postmortem (Raunio et al. 1979).

2.6.6 Evolution of ECG changes after myocardial infarction

The myocardial necrosis induced changes in the ECG are instable. Within a 2 year period 10% of anterior and 25% of inferior MIs loose their diagnostic ECG pattern (Sheifer et al. 2001). In MI survivors 4 years after the MI approximately 20% show normal ECG findings (Sheifer et al. 2001). A substantial proportion of the Q waves following MI disappear with elapsing time. Total Q-wave regression has been shown to occur in 42% and partial regression in 13% following Q-wave MI (mean follow up 8.3 years). This regression of Q waves was unrelated to the location of MI, future survival or future reinfarction (Marcus et al. 1989). During a 1-4 year period following MI the Q wave changes have shown to disappear in 5.6%, but ST-T changes following MI in 54.4% of the patients. In this study either, no relation between the disappearance of the MI signs in ECG and MI location or the frequency of future reinfarction was observed (Cox 1967). In a study by Kaplan et al. (Kaplan et al. 1964) during a mean of 3.4 years of follow up 15% of the Q-wave MIs showed total regression of the Q waves with a mean time of 1.6 years to the disappearance of the changes. Again, no relation was found with respect to the MI location and future survival.

In study, with LVEF assessed with radionuclide ventriculography, in 16% of the patients with QMI the ECG signs of MI completely disappeared within 6 months of follow up. In patients with NQMI 11 of 12 showed complete regression of ECG signs of MI. In inferior MI the disappearance of Q waves was more frequent than in anterior MI, but no relation to size of MI and disappearance of MI signs in ECG was found (Bergovec et al. 1993).

After MI remodeling of LV is related to cardiac electrical instability. Markers of both phenomena predict sudden death after MI (Gaudron et al. 2001). During the first week after the MI the incidence of late potentials increases, whereas during the first year after MI the filtered QRS duration decreases (Simson 1990).

2.7 Body surface potential mapping (BSPM)

Body surface potential mapping is a technique of recording electrocardiograhic potentials with unipolar torso leads over wide thoracic areas. BSPM has several advantages as compared to the conventional 12-lead ECG. Owing to the abundant recording locations it has higher spatial information content. In addition to being suitable for extracting the dipolar information content (reduction of the BSPM data to a single moving dipole source responsible for the body surface potentials; global content) from BSPM recordings, it contains more information on the nondipolar (those electrical components unable to fit into the dipolar model, local content) components of the electrocardiogram than the conventional 6 chest leads (Medvegy et al. 2002). Vectorcardiography makes the assumption of a dipolar source, whereas BSPM emphasizes the detection of local events (Mirvis 1987). Since a potential at any torso site may be derived from an infinite number of sources, a dipolar model is unsatisfactory. If the dipolar model were the true solution to the inverse problem, all the electrocardiographic information could be recorded from 6 chest leads (Mirivs 1987). When solving the inverse problem with regard to intracardiac sources, the body surface potentials can yield multiple source configurations, while for epicardial potentials it is possible to obtain a unique solution from the body surface potentials (MacLeod et al. 1995, Yamashita 1982). The multipolar analysis of BSPM is the spatial analog of frequency analysis (Flowers and Horan 1995). The body surface potential distribution may be decomposed into series of electrical sources with increasing complexity, at the center of an enclosed surface, the first of which is a dipole, the second is a tetrapole, the third is a ocatapole and so on (Flowers and Horan 1995). The potential recorded on the body surface is dependent on the distance of the source, the heart, from the recording site. The potential declines approximately in proportion to the square of the distance, thus decreasing the nondipolar components of ECG with increasing distance from the source (Surawicz 1995c).

BSPM collects clinically important information from body areas uncovered by the standard V1-6 leads. In addition to the temporal and intensity components of electrocardiographic signals, BSPM emphasizes the spatial aspects of the signals, a characteristic unique to BSPM (Mirvis 1987). Positivity on a body surface map indicates an activation wavefront moving towards the measuring electrode (Medvegy et al. 2002). BSPM techniques have been available since 1960s. Due to the abundant information in BSPM it requires computer processing for interpretation. Several numbers and combinations of unipolar chest leads have been used (Medvegy et al. 2002). The postprocessing of the recorded signals also varies greatly from study to study. The visual display of the results is generally in the form of torso maps: isopotential maps, displaying at a given time instant potentials of the same magnitude connected by a line; isointegral maps, displaying isointegral lines of a time-voltage integral during a given time period; and departure maps, displaying a map of a single patient or a group of patients deducted from an average map of a group of healthy controls. In addition, more unusual map displays may be used, as isochrone maps displaying sites activated at the same time, or discriminant index maps displaying differences between a control group and a study group

as discriminant indexes (DI) proportional to t-value and identifying those torso areas with statistically most significant differences between the two groups.

The maps and signals may be analyzed in very heterogeneous ways. They can be visually compared, at different time intervals, with respect to different parameters (instantaneous amplitudes, integrals). They can be compared to what is considered as normal maps with respect to areas of abnormal negativity or positivity, with respect to the temporal and/or spatial appearance of abnormal potentials, with respect to distance or angle between map maxima and minima etc. (Medvegy et al. 2000, Ackaoui et al. 1985). Analysis of the maps may also be based on feature extraction and spatial and/or temporal comparison of single parameters in one or several BSPM leads and models can be constructed of combinations of these parameters for future analyses. Many BSPM studies have displayed their results in complex, descriptive map forms, which are difficult to interpret and to adopt and therefore unlikely to gain wider clinical use (Tseng et al. 1999, Ishikawa et al. 1988, Medvegy et al. 2000).

BSPM has been studied in the various clinical presentations of myocardial ischemia and infarction since the 1970's. BSPM provides greater diagnostic information than 12-lead ECG for prior MI (Ackaoui et al. 1985, Ambroggi et al. 1986, Kubota et al. 1985, Medvegy et al. 2000) and acute MI (Kornreich et al. 1993, McClelland et al. 2003, Menown et al. 2000a, Menown et al. 2001, Montague et al. 1986, Montague et al. 1983). The BSPM maps have reported, even, to detect stable coronary artery disease in a resting, painfree state with a sensitivity and specificity greater than 94% (Green et al. 1987).

2.7.1 Distribution of BSPM variables in healthy subjects

Mean normal BSPM maps of the QRS (QRS onset to J-point) and STT (J-point to end of T wave) integrals show a zero line running approximately from the left shoulder to the right abdomen with positive values on the left anterior thorax. The difference between the depolarization and repolarization maps is mainly in the intensity of the isocurves, with greater intensity on the depolarization map. The QRST map shows a similar pattern (Flowers and Horan 1995, Montague et al. 1981). The QRSSTT (QRS onset to end of T wave) isointegral map is referred to as the ventricular gradient map (Medvegy et al. 2002). Men show greater maximum and minimum time integral values than women (Montague et al. 1981). Serial variability in time integral maps of normal subjects is greatest for parameters reflecting repolarization, including the QRST time integral (Montague et al. 1981). The QRS and ST-T potentials decrease with increasing age. During the QRS only minor differences occur between men and women in amplitude and distribution, whereas men show greater T potential amplitudes (Green et al. 1985).

2.7.2 BSPM in prior MI

The sensitivity for the detection of prior MI is higher for BSPM than for the standard 12-lead ECG. BSPM detects electrocardiographic abnormalities in patients with prior MI but

non-diagnostic 12-lead ECG (Mirvis 1987). In patients without changes in the 12-lead ECG, 73-83% showed abnormalities in BSPM maps (Hirai et al. 1984, Osugi et al. 1984, DeAmbroggi et al. 1986). Distinction between patients with an intraventricular block and MI is possible with BSPM (Mirvis 1987).

BSPM has revealed electrocardiographically distinct patterns between patients with prior MI exclusively in inferior location and in those with right ventricular involvement, indicating the ability of BSPM in estimating the size of MI (Montague et al. 1983). Serial BSPMs after acute MI were studied with a departure-map technique. The departure areas decreased during a period of 1 week to 2 months after MI. The departure areas correlated with the extent of MI determined by radionuclide ventriculography and thallium-201 single photon emission tomogram one month after MI, and had a negative relation with LVEF (Cahyadi et al. 1989). Three electrocardiographic methods, BSPM, 12-lead ECG, and vectorcardiography, and thallium-201 were compared with left ventriculography in post MI patients for correlation with segmental localization and degree of asynergy. BSPM had the highest correlation with left ventriculography (r=0.88), followed by 12-lead ECG, vectorcardiogram, and last Thallium-201 (r=0.55) (Ackaoui et al. 1985). QRS isointegral maps, using departure area technique, have demonstrated good correlation of departure area (of more than 2 SD) and LVEF (r=-0.93) and the extent of asynergy (r=0.74) in patients with prior anterior MI (Kubota et al. 1985). Furthermore, QRS isointegral departure areas correlate with a defect score of thallium-201 myocardial perfusion imaging in patients with prior anterior MI (r=0.88) and prior inferior MI (r=0.79), but not in patients with coexisting anterior and inferior MI (Tonooka et al. 1983).

However, Kittnar et al. found only limited accordance in BSPM repolarization maps, ST-segment isoarea maps and ST-segment isointegral maps, with dyskinetic ehco or ventriculographic findings in patients with CAD (Kittnar et al. 1993).

Montague et al. have in 1989 concluded that myocardial ischemia is a heterogenous process with temporal continuum and has predicted that quantitative BSPM variables will become important in the grading of ischemia and estimating patient prognosis (Montague and Witkowski 1989).Serial BSPMs (3 days and 8 months post MI) were compared by means of subtracting the initial form follow-up group mean map. The temporal changes in the Q-zone time-integral maps were small, in contrast with marked changes in the ST-segment time-integral maps that approached the normal ST-segment time integral maps at follow-up. The authors conclude that the Q-zone reflects irreversible myocardial injury, whereas the ST-segment identifies the area at risk, which stabilizes over time (Montague et al. 1984).

2.7.3 BSPM in acute ischemia

For the detection of STEMI in chest pain patients, BSPM has proved more sensitive (90% vs. 76%) and of similar specificity (97% vs. 98%) to the 12-lead ECG (Ornato et al. 2002). BSPM has also detected ST elevation over the right ventricle and posterior wall in patients with inferior AMI more often than the 12-lead ECG with 4 additional leads (Menown et al. 2000a).

In UAP/NSTEMI patients early invasive treatment affords benefit over conservative management, but thrombolysis has no beneficial effect and may even be harmful (TIMI investigators 1994). ST depression in 12-lead ECG may occur in UAP, NQMI (true non STEMI), or as reciprocal changes in STEMI not covered by 12-lead ECG. In the latter group fibrinolytic therapy might be beneficial (Self et al. 2006).

BSPM showed ST elevation with 71% sensitivity and 53% specificity for AMI in patients presenting only with ST depression in the 12-lead ECG (Menown et al. 2001). In patients with ST depression only in the initial 12-lead ECG, a multivariate model constructed from BSPM leads and parameters, requiring the whole BSPM lead set, identified MI better than the 12-lead ECG, whereas univariate ST elevation BSPM parameter, in any lead, failed in comparison with the 12-lead ECG (Menown et al. 2001). In a recent study BSPM in the setting of acute myocardial ischemia has shown greater sensitivity (47% vs. 40%) but lower specificity (86% vs. 94%) relative to the 12 lead ECG, in both high and low to moderate-risk patients. The clinician's interpretation of the BSPM would therefore result in a clinically significant overdiagnosis of MI (Carley et al. 2005).

In acute MI, with the location determined by radionuclide imaging, a stepwise statistical procedure identified a pair of BSPM leads for each MI location for the ST deviation parameters (depression and elevation), in which the optimal detection of MI could be obtained (Kornreich et al. 1993). In this statistical procedure at a specificity level of 95% sensitivities of 82%, 100%, and 93% were obtained for anterior MI, inferior MI and posterior MI, respectively. Prospectively testing these parameters in lead pairs is, though, yet to be done. However, this work demonstrates the superiority of BSPM over the standard 12-lead ECG, since five of these six leads lay outside the standard chest leads. They also demonstrated that ST depression in each MI group is more deviant from normals than ST elevation, signifying, again, the importance of ST depression.

An algorithm derived from BSPM containing 14 variables, requiring the whole BSPM lead set, has shown sensitivity of 96.6% with a specificity of 100% in a prospective set of patients with acute MI and healthy controls (McMechan et al. 1995). A major shortcoming of this study was that the criteria for the diagnosis of AMI was not defined, and might even be based on the 12-lead ECG.

Another multivariate BSPM derived model produced as prospectively tested sensitivity of 96% with a specificity of 77.4% for acute MI detection (Menown et al. 1998). Again, weakness of this study was that the diagnosis of AMI, for reference, was based on WHO criteria from 1979 (WHO Task Force 1979), where the diagnosis could be made by symptoms and ECG criteria only, so no direct comparison with the 12-lead ECG could be made.

An automated BSPM algorithm has proved superior to the physician's interpretation in sensitivity (64% vs. 45%) with the same specificity (94%). The BSPM algorithm improved the diagnostic sensitivity by 1.4 compared with the physician (McClelland et al. 2003). The physicians' diagnosis was, however, based solely on ST elevation. In addition, the time points were manually marked before the application of the complicated, multivariate algorithm.

BSPM has also been studied in estimating reperfusion after thrombolytic therapy (Menown et al. 2000a). In 33 patients receiving thrombolysis for acute MI, a model containing 28 BSPM variables, and requiring the whole BSPM lead set, achieved 97% sensitivity with 100% specificity, as compared with 12-lead ECG ST-resolution achieving 59% sensitivity and 50% specificity.

The loss of mirror image in BSPM improves the diagnosis of acute MI in patients with LBBB as compared to 12-lead ECG criteria for AMI and LBBB (Maynard et al. 2003). Sensitivity for detecting AMI with LBBB by the 12-lead ECG criteria was only 33% with a specificity of 97%, as opposed to the sensitivity of 67% and specificity of 71% the loss of mirror image in BSPM.

BSPM during PTCA induced ischemia identifies ischemia more readily (54%) than 12-lead ECG (18%) as judged by ST segment alteration from pre-procedure state to the one during balloon inflation (Maynard et al. 2004). A method for the presentation of color maps for ST 60 changes during balloon inflation has shown characteristic changes for each of the culprit arteries (Carley et al. 2004). A model calculated from BSPM recorded before and during PTCA balloon inflation is able to predict the site of ischemia produced by the inflation (MacLeod et al. 1995). A discriminant function analysis of QRS and ST-T isointegral maps in acute MI has shown sensitivity of 72% for anterior and 76% for inferior MI (site electrocardiographically determined, enzyme rise required), with a specificity of 97% (McMechan et al. 1994).

In a simultaneous recording of epicardial and BSPM potentials in porcine hearts the occlusion of LAD caused increase in epicardial QRST integral values at 20 seconds of occlusion and increase in BSPM QRST integral values at 40 seconds of occlusion. Both the magnitude and area of positivity of QRST integral increased during occlusion (Nash et al. 2003).

Prehospital BSPM recordings in chest-pain patients have shown to detect enzymatically verified AMI with a sensitivity of 80% and a specificity of 92%, as opposed to the 12-lead ECG with a sensitivity of 57% and a specificity of 94%, when ST elevation at the J point in both was used as AMI criterion (Owens et al. 2004).

In the acute phase of MI, BSPM variables have demonstrated only very modest correlations with other techniques measuring MI size (McPherson et al. 1985).

In patients with CAD, without previous MI, even at rest, the BSPM methods have revealed abnormalities in isopotential T wave maps, distinguishable also from the maps of patients with LV overload, though these are purely descriptive and complicated to interpret (Ishikawa et al. 1988).

Maximum ST-segment deviation registered with BSPM in the setting of acute inferior (location determined with 12-lead ECG) MI has shown to correlate with long term mortality and morbidity. While the correlation also applied, to a lesser extent, to ST-segment depression in the standard 12-lead ECG, it was found, however, that the standard chest leads lie over an area of steep voltage gradient. Therefore, even small lead displacements can lead to large changes in the ST-segment, distorting the interpretation about ischemia (Walker et al. 1987).

The ST-segment alterations detected by BSPM during PTCA are in agreement with those observed during spontaneous acute ischemia, whereas demand-type ischemia

induced during exercise testing shows dissimilar distributions of ST-segment changes, due to the subendocardial nature of ischemia (Horacek and Wagner 2002). In exercise stress testing of CHD patients the BSPM has shown to be able to identify the culprit artery and to detect ischemia indifferent to its location or the presence of prior MI (Farr et al. 1987, Nakajima et al. 1988, Kubota et al. 1989, Hänninen et al. 2001).

2.7.4 Optimal recording locations for detecting myocardial ischaemia

Kornreich et al. (Kornreich et al. 1993) identified three pairs of leads for the detection of acute MI for each MI location, using ST depression and ST elevation as variables. Anterior MI was best detected above V2 (ST elevation) and on lower left back (ST depression); inferior MI was best detected on right abdomen (ST elevation) and in left shoulder region (ST depression); and posterior MI was best detected on lower back (ST elevation) and in left shoulder region (ST depression). All were outside the standard precordial leads. The same electrode sites and lead measurements are valid during balloon inflation induced ischemia (Kornreich 1998).

Horacek and Wagner propose, based on previous research, three bipolar chest leads for the detection of acute myocardial ischemia induced by the occlusion of the three main coronary artery branches (Horacek and Wagner 2002). These locations are based on ST60 amplitude parameter studies. For LAD occlusion the proposed lead pair is one with the positive terminal near V3 and a negative terminal below posterior lead V8; for RCA occlusion one with the positive terminal in proximity of left iliac crest and the negative terminal above V3; for LCX occlusion one with the positive terminal below posterior lead V8 and a negative terminal close to V2. The estimated sensitivity for these bipolar leads for ischemia detection would be 95%, 79%, and 82% for LAD, RCA, and LCX occlusion induced ischemia, respectively (Horacek et al. 2001). These bipolar leads can be derived form the standard 12-lead ECG or from a 4-lead EASI system (Dower et al. 1988) and the estimated performance for ischemia detection is similar to the bipolar leads (Horacek et al. 2001).

In a study comparing unipolar BSPM leads to bipolar Holter leads for detecting ischemic ST elevation during balloon inflation a poor correlation was found between the two. Best unipolar BSPM leads for the detection of ischemic ST elevation were below V2 for LAD occlusion, right abdomen for RCA occlusion, and just to the left of sternum, between the 4th and 5th intercostal space for LCX (Fuller et al. 1996). The reason for poor identification of the bipolar Holter leads V_2 and V_5 is that the potential recorded by a bipolar lead corresponds to the potential difference between a unipolar lead pair. Thus, no change in potential is observed if the potential change recorded by the electrodes of the bipolar pair is the same (Fuller et al. 1996). This is a major shortcoming with bipolar Holter recordings for the ST-segment shift detection. Ischemic changes may, however, become visible if the location of the electrodes of the bipolar pair is suitable with regard to the ischemic area.

2.7.5 Optimal recording locations for detecting myocardial infarction scar

In a study of 177 patients with prior MI (in 39 patients less than 1 week) Kornreich et al. found a combination of 6 features in 3 recording locations to detect MI with a sensitivity and specificity of 95%. The three optimal leads were aVF, a lead below the right clavicle, and a lead on the left dorsal flank. The optimal features were instantaneous amplitudes of time normalized QRS and STT waves. The STT measurements accounted for most of the separation (Kornreich et al. 1985). In another study by Kornreich et al. (Kornreich et al. 1991) a combination of 6 features at 6 recording sites produced a specificity of 96% and a sensitivity of 94% for the detection of prior MI, old and recent. These features were instantaneous amplitudes of time-normalized PQRST waveforms and the durations of these waveforms. The six optimal recording locations were in the right subclavicular area, right inferior flank, to the right of V1, two on the left dorsal flank, and mid back. This model was further tested in acute QMI and NQMI and found to correctly classify 93% and 91% of them, respectively.

In a study with combination of 6 features consisting of time normalized instantaneous amplitudes of the QRS and ST-T waves sensitivity of 97% and 94% was achieved at a specificity level of 95% for anterior and inferior MI, respectively. These figures exceeded the ones produced from the simultaneously recorded 12-lead ECG. The optimal locations for recording variables for anterior MI were right subclavicular region, upper abdomen, upper left chest, left flank, and mid back; for inferior MI right subclavicular region, lower right flank, above V4 and V5, left leg, lower left back and back of the neck. A shortcoming was that the MI location was determined electrocardiographically (Kornreich et al. 1986).

3 AIMS OF THE STUDY

The aim of the studies included in this thesis was to improve the relatively poor diagnostic capability of the ECG, at present, in prior MI and evolving myocardial ischemic injury.

The method of choice in the studies was BSPM, which is able to detect practically all information available on body surface of heart's electrical activity. BSPM, however, is unpractical and time consuming in everyday diagnostics. Therefore the goal was to find the optimal recording locations and optimal ECG variables for ischemia and MI diagnostics. We sought for simple, quantitative ECG variables, functional in a drastically reduced set of leads, for the detecting, grading, and localizing of myocardial infarction scar and evolving myocardial ischemic injury.

The ultimate objective is to develop an automatically applicable method for screening purposes for prior MI and for monitoring and therapeutic decision-guiding purposes in acute ischemia.

4 MATERIALS AND METHODS

4.1 Study subjects

In total 144 patients with prior MI, 79 patients with evolving ischemic insult or injury, 42 patients with LVH, and 84 healthy controls were included in the studies. All of the study subjects gave their informed consent. The research protocols were approved by the local ethics committee and complied with the Declaration of Helsinki.

4.1.1 Studies I and II

In the studies I and II the same study subject population was examined: 24 patients with coronary artery disease and 24 healthy controls (Table 2.). All of the patients had a history of one or more remote (range 1.5 months to 17 years) MIs and angiographically verified coronary artery disease. Of the 24 patients, 20 had a triple-vessel disease, 3 had a two-vessel disease, and 1 had a single-vessel disease. All of the patients underwent CE-CMR for the localization of MI (Table 3.). QMI, according to Minnesota code in the 12-lead ECG, was found in 11 patients. According to the Sokolow-Lyon criterion (SV1+RV5/V6), mild left ventricular (LV) hypertrophy was observed in 7 patients (3.6-4.1 mV) (Sokolow and Lyon 1949). None of the patients were known to have a condition affecting repolarization, e.g. long QT-syndrome, nor were they taking drugs able to influence repolarization.

The healthy controls had no history of heart disease, and had normal results in exercise ECG and in rest echocardiography.

The study subjects had no bundle branch or fascicular block in 12-lead ECG.

Table 2. *Characteristics of study groups in studies I and II*

	Patients	Controls	P value
Number of subjects	24	24	
Male/Female	21/3	18/6	
Age (years)	62 ± 9 (range 46-82)	52 ± 10 (range 29-67)	0.001
Duration of QRS (ms)	97 ± 10 (range 81-116)	92 ± 7 (range 76-101)	0.058
LVEF (%)	49 ± 14	66 ± 7	< 0.001

Mean ± standard deviation. LEVF = left ventricular ejection fraction. P value for the difference between the patient and the control group is shown in the right column.

Table 3. *Patient classification according to the myocardial infarction location in studies I and II*

Infarction group	Number of patients	QMI/NQMI	Age (years)
Anterior	10	6/4	63 ± 11
Lateral	5	2/3	60 ± 9
Inferior	11	6/5	65 ± 8
Posterior	11	7/4	66 ± 9
Apical	12	8/4	63 ± 10

Mean ± standard deviation. A patient can be assigned into more than one group. NQMI = non Q-wave myocardial infarction, QMI = Q-wave myocardial infarction.

4.1.2 Studies III, IV, and V

In the studies III-V data was obtained from 144 angiographically verified coronary artery disease patients, with at least 1 prior MI in the hospital records, participating in studies on ventricular arrhythmia risk analysis in old and in recent MI (Korhonen et al. 2002, Korhonen et al. 2006). The study subjects in studies I-II were included.

Local LV dysfunction was determined by echocardiography (36 patients), cine-angiography (68 patients), or both (40 patients), along with LVEF. The LV dysfunctional region was anterior in 66, inferoposterior in 89, and lateral in 15 patients. The patients were diagnosed, on the basis of the 12-lead ECG, as having a QMI or a NQMI, according to the Minnesota criteria 1-1. MI was defined as old (>6 months) or recent (4 days to 1 month).

As controls were recruited 75 healthy volunteers with no history of symptoms or signs suggestive of coronary artery disease. They were examined with rest ECG and stress ECG or rest echocardiography, showing normal findings.

None of the study subjects had a bundle branch block or hemiblock, chronic atrial fibrillation, or cardiac pacemaker.

Study subject characteristics are presented in Table 4.

Table 4. *Characteristics of study population in studies III-V*

	N	Age (years)	LVEF (%)	BMI	Sex F/M	QRS duration (ms)	QT duration (ms)
All Patients	144	61±10	41.0±9.9	27.0±4.2	27/117	105±18	407±38
Recent MI	59	59±10	42.1±7.9	26.7±4.0	13/46	99±18	412±42
Old MI	85	62±9	40.2±11.1	27.2±4.3	14/71	110±17	403±36
QMI	97	60±9	39.9±9.2	27.4±4.2	17/80	107±18	407±39
NQMI	47	63±10	43.3±11.0	26.2±4.2	10/37	102±16	407±37
Controls	75	52±12	61.8±7.3	25.8±3.9	19/56	97±12	392±33

Significant differences between the groups for subject age, LVEF, BMI, QRS duration, and QT duration were found between all patients and controls ($p<0.05$), and between Old vs. Recent MI in QRS duration ($p<0.001$).
BMI=Body mass index, F=Female, LVEF=Left ventricular ejection fraction, M=Male, MI=Myocardial infarction, N= Number of subjects, NQMI=Non-Q-wave myocardial infarction, QMI=Q-wave myocardial infarction.

4.1.3 Study VI

In the final, prospective study the 79 chest-pain patients, with ST-segment abnormalities in the initial 12-lead ECG suggestive of myocardial ischemia were recruited at the Helsinki University Central Hospital emergency department (ED). The clinicians' initial 12-lead ECG interpretation was ST elevation in 57 patients and non-ST elevation in 22 patients. Prior myocardial infarction was present in 13 of the patients.

Patients were grouped according to whether they suffered myocardial damage (AMI) or not (UAP). CK-Mb mass>5 ug/l was considered a sign of myocardial infarction. Nearly all of the patients (76) underwent coronary angiography. All of the UAP patients showed significant stenoses in the coronary angiography. The patients were grouped according to culprit artery stenosis. Left anterior descending (LAD) was the culprit artery for 32 patients, right coronary artery (RCA) for 26 patients, and left circumflex coronary artery (LCX) for 10 patients. All of the patients had echocardiography performed acutely, within 12 hours from the onset of pain, to determine LVEF.

As controls were recruited 84 healthy volunteers with no history of symptoms or signs suggestive of coronary artery disease. They were examined with rest ECG and stress ECG or rest echocardiography, showing normal findings. The healthy controls in studies I-VI were included.

As an additional comparison group 42 patients with left ventricular hypertrophy (LVH) were analysed (Oikarinen et al. 2004). The LVH patients had aortic valve stenosis or arterial hypertension and the LVH was diagnosed by echocardiography. They had no signs of coronary artery disease, no left ventricular dysfunction, and no pathological Q-waves in the 12-lead ECG.

None of the study subjects had bundle branch block, atrial fibrillation, or pacemaker. The study subject characteristics of study VI are presented in Table 5.

Table 5. *Baseline characteristics of the study subjects in study VI*

	Number of subjects	Sex F/M	age	BMI	LVEF	CK Mb max
Controls	84	18/66	53±13	25.7±3.7	>50	
LVH patients	42	17/25	63±12	26.3±3.6	>50	
Ischemia patients	79	22/57	61±11	27.5±54.4	53±10	147±193
AMI	68	18/50	61±11	27.6±4.4	52±10	171±198
UAP	11	4/7	62±10	26.5±4.3	60±6	3±1

AMI=acute myocardial infarction, BMI=body mass index, CK=creatine kinase, F=female, M=male, LVEF=left ventricular ejection fraction, LVH=left ventricular hypertrophy, UAP=unstable angina pectoris

4.2 BSPM recording and data processing

In studies I-V resting BSPM for 5 minutes was recorded with 120 unipolar leads covering the whole thorax, and with 3 limb leads. Wilson's central terminal was used as a reference potential for all the chest leads. The electrodes were mounted on 18 strips, placed on the subject's thorax vertically with horizontal spacing determined by the dimensions of the upper body (Figure 7.).

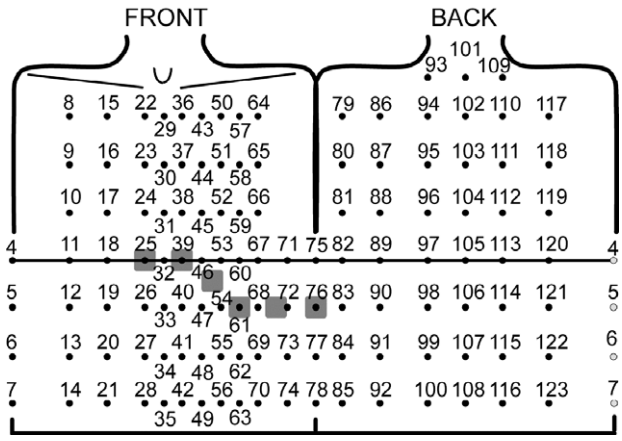

Figure 7 *Body surface potential mapping (BSPM)-layout. Displayed on the left is the front of the torso and on the right the back of the torso. Black dots represent the BSPM electrode sites. The grey squares represent the 12-lead electrocardiogram chest leads. The horizontal line runs through the 4th intercostals space on the sternal level.*

The BSPM data were visually inspected for validity of the recording, and signal-averaged according to criteria of 0.9 or greater correlation of the QRS complex to a selected template beat and maximum noise of 50 uV. The baseline was defined from a 20 ms section of the PQ segment (studies I-II) or TP segment (studies III-VI) and estimated by the 3rd order spline function fitted to consecutive PQ segments (study VI). Invalid leads were replaced by interpolation of data from surrounding leads. The QRS onset and offset were determined automatically from the vector magnitude of a representative set of high-pass filtered leads. QRS was divided into 6 and 4 temporally equal segments. T-wave apex and end were determined automatically for each lead separately. The median of T-wave end of all leads was used for calculations of time integrals and time intervals. STT segment was defined as the time interval from the QRS offset to the T-wave offset. The J-point was determined for each lead separately as the time instant of the maximum curvature of the signal returning to the ST-level around the QRS offset.

Time integrals were calculated for the whole QRS, covering depolarisation, and for the QRS sextiles, quartiles, and for the STT segment, comprising repolarisation. QRSSTT integral and its absolute value [QRSSTT integral] represented the integral over the depolarisation-repolarisation phase, i.e. the sum of the QRS and the STT integrals (Figure 8.). This was named QT integral in study VI. Variables containing repolarisation will be referred to as repolarisation variables, even though the QRSSTT integral also includes a depolarisation component.

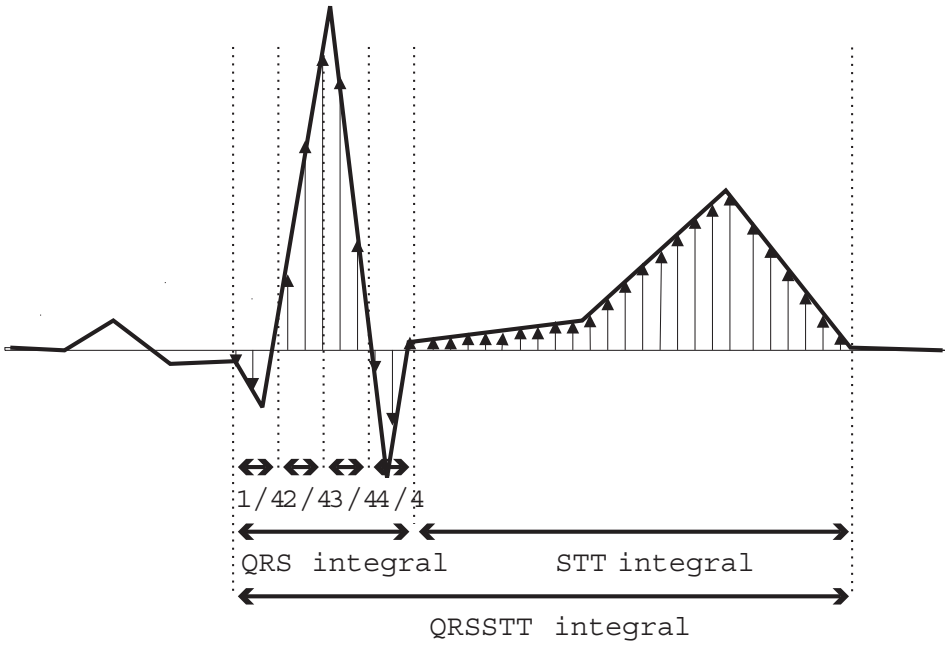

Figure 8 *Display of the electrocardiographic integral variables. The vertical dotted lines represent the QRS onset, the end of the 1st, 2nd, and 3rd QRS quartiles, the QRS offset, and the T-wave offset, respectively. The solid vertical lines starting from the horizontal baseline and ending with an arrow demonstrate the area and sign of the integral values.*

4.3 Discriminant index analysis

Discriminant indexes (DI) were used to identify the optimal recording locations to separate patients from the controls and different patient groups from one another. DI was calculated as described by Kornreich et al. (Kornreich et al. 1991). The mean value of group A was subtracted from the corresponding mean of group B. The difference was divided by the pooled standard deviation (SD) of the both groups.

The DI value is directly proportional to the t-value in the Student's t-test, indicating the difference between the groups relative to the standard deviation of the study population. With fixed group sizes, the greater the absolute DI value ([DI]), the better the ability of the lead to differentiate between the groups. Negative DI values indicate higher mean values for group A and positive DI values higher mean values for group B.

The optimal lead was thus identified by a lead producing the greatest absolute DI value. Furthermore, the positive DI values indicated higher and negative DI values lower parameter values for the patients than for the controls (usually group A corresponded to controls and group B to patients in these studies) .

4.4 Map display

In study I isocontour maps were drawn for the optimal average QRS sextile time integral in each MI group and in the control group, and for the corresponding DI values. For visual inspection, the isocontour maps were divided into four quadrants on the anterior torso.

In study II isocontour maps were constructed for the average QRS and STT time integrals, in MI patients and controls, and for the corresponding DI values.

In study V isocontour maps for the group average QRSSTT integral were displayed, separately for anterior MI group, inferoposterior MI group, apical MI group, and the controls.

In study VI isocontour maps were displayed for the group average QT integral (=QRSSST integral) for the ischemic patients and for the controls.

4.5 Statistical analysis

The significance of difference between the study groups was determined by the Mann-Whitney U-test, which does not presume equal variances. Correlations between the parameters were examined with Pearson's correlation coefficient (r). A two-tailed p-value ≤ 0.05 was considered statistically significant. Receiver operating characteristic (ROC) curves were created to assess the performance of the parameters in the optimal leads, as judged by DI-value. The results are given as the area under ROC curve (AUC%) with 95% confidence interval (CI). AUCs were statistically compared by a method presented by Hanley and McNeil (Hanley and McNeil 1983). The SPSS (Inc., Chicago, IL, USA) for Windows (version 10.0) biostatistics software was used.

5 RESULTS OF THE STUDIES

5.1 Diagnostic performance of the electrocardiographic variables

5.1.1 QRS segment time integrals: sextiles and quartiles (I, IV, V, VI)

The time sextile integrals of the QRS complex showed different MI detection capability depending on the MI location. The optimal sextile for each MI location group was chosen to be the one with the greatest number of leads with absolute DI value exceeding 1. For the different MI locations, the lateral, anterior, inferior, posterior, and apical, the optimal sextile integrals were the 1st to the 5th, respectively (Table 6., Figure 9.). The best AUCs, in each MI location, ranged from 83% to 90% during the optimal sextiles. All of the optimal leads lay outside the standard 12-lead ECG (I).

Table 6. *The optimal sextile integrals of the QRS and the corresponding optimal recording sites in MI patient groups. P-values for the difference between MI group and the controls are shown (I).*

Infarction group	The optimal sextile	The optimal chest area	AUC (%) of optimal lead	p-value
Lateral	1st	left 4th intercostal	83	0.024
Anterior	2nd	right inferior	83	0.002
Inferior	3rd	mid inferior	83	0.002
Posterior	4th	left inferior	84	0.001
Apical	5th	right superior	90	< 0.001

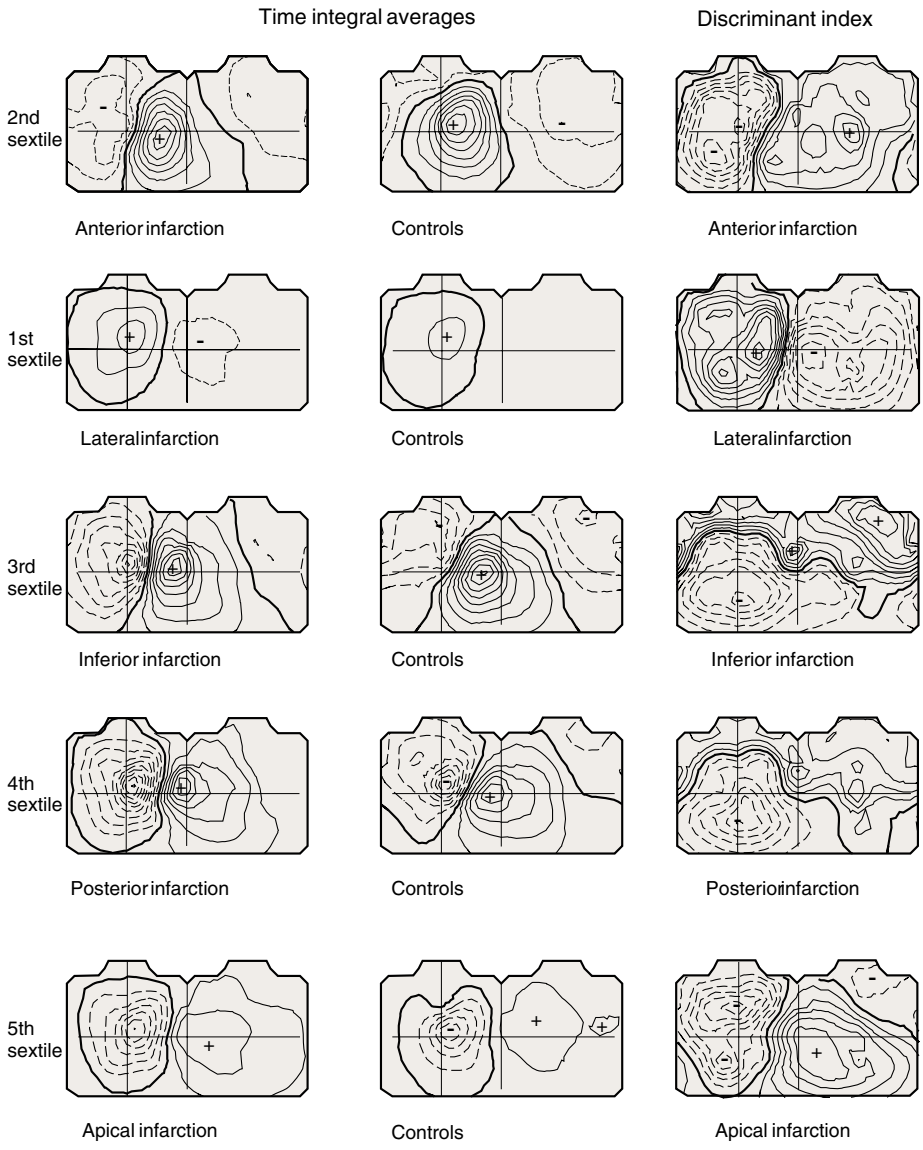
Time integral averages
Discriminant index
2nd sextile
Anterior infarction
Controls
Anterior infarction
1st sextile
Lateral infarction
Controls
Lateral infarction
3rd sextile
Inferior infarction
Controls
Inferior infarction
4th sextile
Posterior infarction
Controls
Posterior infarction
5th sextile
Apical infarction
Controls
Apical infarction

Figure 9 *Isocontour maps of the group average time integral values, and the corresponding discriminant index (DI) values, of the optimal QRS sextiles for each of the myocardial infarction location subgroup. Visually, the average time integral maps of the infarction group and the control group are not distinct, whereas the DI maps are divergent for each infarction patient group. The area with the highest density of DI contour lines is the area for the optimal detection of infarction. The vertical and horizontal lines mark the borders of the quadrants on the anterior torso. The thick solid line = zero line, the thin solid line = positive values, dashed line = negative values. The isocontour step is 1.0 mVms for the anterior, lateral, and inferior infarction patient groups and for the corresponding sextiles in the control group, and 2.5 mVms for the posterior and apical infarction groups and the corresponding sextiles in the control group. The isocontour step is 0.2 for the DI maps.*

In the larger patient population (144 patients) analysis of QRS integral quartiles revealed that of the QRS quartile integrals the first two operated best in detecting prior MI. In all the MI locations, the AUC of the optimal lead for the 2nd quartile integral was the largest, 87% (CI 83-92%), followed by the AUC of the 1st quartile integral, 81% (CI 75-87%). The AUC of the 2nd quartile integral exceeded that of the 1st quartile ($p = 0.05$). Additionally, weak correlations were found with 2nd quartile and LVEF in 72 leads, with strongest correlation in lead 47 ($r = 0.42$, $p < 0.001$).

When analyzed according to the MI location, the 2nd QRS quartile integral showed AUCs exceeding 90% for the anterior and lateral MI, and 86% ($p < 0.001$) for the inferoposterior MI, in groups with MI in single or multiple locations. Subgroups with MI in a single location only showed even higher AUCs (Table 7.)

The 1st QRS-integral quartile distinguished between the solitary anterior and the solitary inferoposterior MI subgroups with an AUC of 91% (CI 85-98%) in optimal location on left lower back (V).

Table 7. *Areas under receiver operating characteristic curves (AUC) for detection of solitary prior myocardial infarction (MI) in the optimal leads. CI = confidence interval. (V)*

	QRS-integral quartile	The optimal chest area	AUC (%) of optimal lead	CI(%) of optimal lead
Anterior	1st	Upper left chest	96	92-100
Inferoposterior	1st	Left scapula	87	80-93
Apical	1st	Lateral to V_2	98	95-100
Anterior	2nd	V_4	92	86-98
Inferoposterior	2nd	Left abdomen	86	79-92
Apical	2nd	Mid abdomen	93	85-100

In the setting of evolving myocardial ischemic injury or insult, the QRS quartile integrals detected ischemia in the order of temporally deteriorating ability from the 1st to

the 4th (AUCs from 79% to 66%). The inclusion of LVH patients in the control group had no substantial effect on the performance of these two variables. During these first two optimal quartiles, the optimal recording locations were on the upper back.

5.1.2 QRS and STT time integrals (II, III, IV,V)

In detecting prior MI the STT integral tended to exceed the QRS integral (Tables 8. and 9.). The STT integral showed, in study II, 92% sensitivity and 71% specificity for prior MI detection. In study IV the sensitivity for MI detection was matched to the Minnesota Q-wave criteria 1-1 of 68%, yielding a specificity of 89% for the STT integral.

The STT integral and the QRS integral performed equally in detecting old and recent MI and QMI and NQMI, but with a tendency for better detection by the QRS integral of QMI and by the STT integral of NQMI. The STT integral showed, with a sensitivity of 92%, specificity of 73% in the detection of QMI and 85% in the detection of NQMI (II).

Additionally, the QRS integral was able, unlike the STT integral, to distinguish between QMI and NQMI.

In study II the optimal location for MI detection for the QRS integral was on the right lower anterior chest and in study IV in its vicinity on the abdomen. The optimal location for MI detection for the STT integral was on the right anterior shoulder in study II, with reciprocal high DI values on the left dorsal flank. In study IV the optimal location for MI detection for the STT integral was and on the left lower flank, in place of standard V6.

Table 8. *The area under receiver operating characteristic curve (AUC) of the optimal lead.(II)*

	QRS integral	STT integral
AUC all patients (%)	83	94
AUC QMI (%)	95	92
AUC NQMI (%)	83	97

Table 9. *AUC and DI of optimal lead for parameters in detection of prior MI (IV)*

	QRS integral	STT integral
AUC all patients (%)	85 (79-90)	89 (84-93)
AUC QMI (%)	87 (82-93)	88 (83-93)
AUC NQMI (%)	80 (72-89)	90 (83-96)
AUC Old MI (%)	83 (77-90)	90 (85-94)
AUC Recent MI (%)	86 (80-93)	88 (82-94)

When the patient population was grouped according to the location of MI (V) the STT integral showed a greater tendency for MI detection in both solitary anterior and inferoposterior MI groups, whereas in the solitary apical MI group the QRS tended to detect MI better (Table 10.). The STT integral distinguished between solitary anterior and solitary inferior MI optimally on mid lower back (AUC of 89%, CI 81-97%).

Table 10. *AUCs for detection of solitary prior MI by use of the optimal leads. CI = confidence interval. (V)*

	AUC (CI) of the optimal lead (%)	The optimal lead location
	STT integral	
Anterior	92 (85-98)	Above V_5
Inferoposterior	93 (89-98)	Below V_6
Apical	91 (82-99)	Above V_5
	QRS integral	
Anterior	88 (81-96)	Above V_3
Inferoposterior	81 (73-90)	Right abdomen
Apical	93 (88-98)	Below V_3

5.1.3 Spatial correlation of the QRS and STT time integrals (II, III, V, VI)

The torso distribution of the QRS integral values in the MI patient and control groups showed similar overall pattern but differed in amplitude. In both groups the QRS time integrals showed positive values over the left lower torso and a zero line running approximately perpendicular to the heart axis. The QRS time integral values were lower for the patients than for the controls (Figure 10.).

The torso distribution of the STT integral values differed between the MI group and the control group. In the controls the map of STT time integral resembled that of the QRS integral, showing similar distribution of the positive and negative areas and zero line, whereas in MI patients the STT time integral showed discordant pattern (Figure 10.).

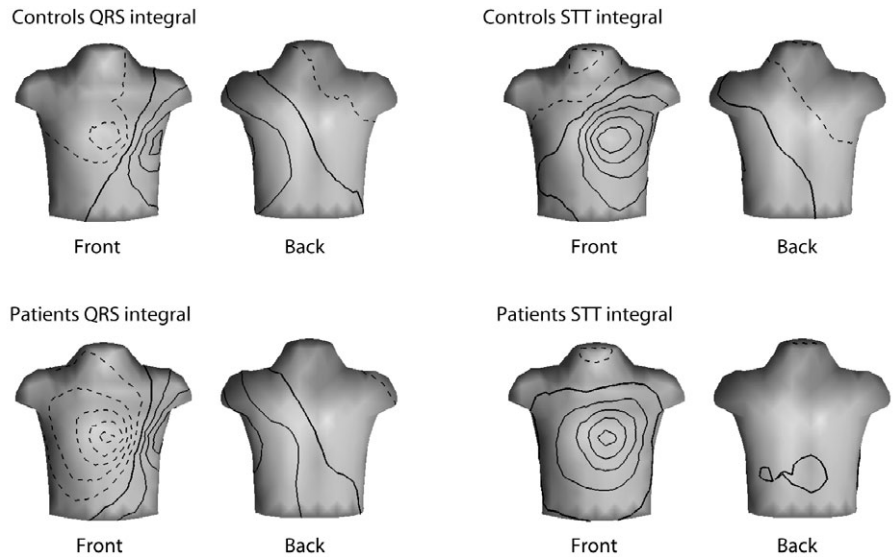

Figure 10 *Isointegral map display of the group average QRS and STT integral values in healthy controls (upper row) and patients with prior myocardial infarction. Contour step 10 mVms in QRS integral maps (left column) and 20 mVms in STT integral maps (right column) (II).*

When plotted according to recording site, the group average QRS integral values correlated negatively with STT integral values in MI patients ($r = -0.58$, $p < 0.001$) and positively in controls ($r = 0.45$, $p < 0.001$). (II)

In the study with larger study subject population (III) in MI patient group the QRS and STT integrals showed even stronger negative correlation on the body surface ($r = –0.901$, $p<0.001$) and positive correlation in the control group ($r=0.285$, $p<0.001$). In subgroup analysis respective correlation was –0.904 for QMI patients ($p<0.001$) and –0.888 for NQMI patients ($p<0.001$). Sensitivity of an inverted QRS/STT relation to detect MI was 79%, as opposed to the sensitivity of the descriptive Minnesota code of 70%. The correlation of QRS and STT integrals was negative in 84 patients in QMI patient group (sensitivity 83%) and in 31 patients in NQMI patient group (72% sensitivity). Furthermore, there was a weak but significant positive correlation between the relationship of QRS to STT integrals and the LVEF ($r=0.219$, $p=0.009$) in MI patients.

The negative spatial correlation of QRS and STT integrals was true also in MI location-based subgroups of patients. In the solitary anterior MI group the correlation between the QRS and STT integrals was –0.60 ($p<0.001$), in the solitary inferoposterior MI group $r = -0.55$ ($p<0.001$), in the solitary apical MI group $r = -0.72$ ($p<0.001$), and in the control group $r = 0.27$ ($p = 0.002$). In the solitary anterior and solitary apical MI groups the scatterplots for QRS and STT integrals, according to chest location, were fairly contracted, whereas for the solitary inferoposterior MI group and for the control group more dispersed. The leads with the most typical relation of QRS and STT integrals for MI,

negative QRS integral and positive STT integral were located on the left flank and included those corresponding to standard V5 and V6.

Also in the setting of evolving ischemic myocardial injury and insult the inversion of polarity of the QRS and STT integrals in ischemia patients held true: the group average QRS and STT integrals showed negative spatial correlation with respect to recording location in the patient group ($r=-0.435$, $p<0.001$), and positive correlation in the control group ($r=0.300$, $p=0.001$) (Figure 11.).

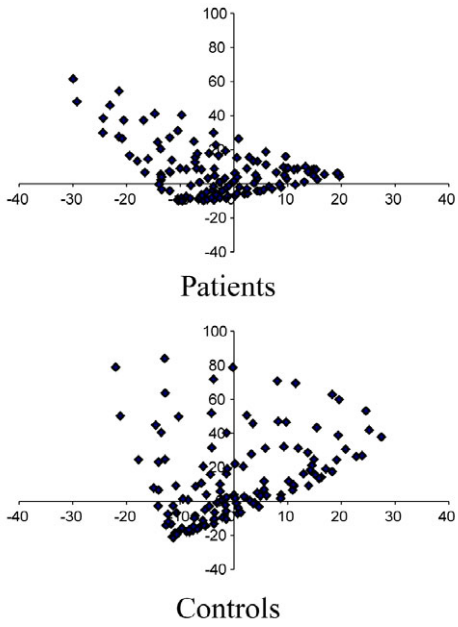

Figure 11 *The group average spatial correlation of QRS and STT integrals in the patients and the controls, i.e., correlation of the QRS integral and STT integral with respect to the recording location on the torso. Each point in the scatterplot represents a group average value of QRS integral (X axis) and STT integral (Y axis) at each single lead on the torso. Values are in mVms (VI).*

5.1.4 QRSSTT time integral and the T maximum amplitude in prior MI (IV, V)

Of all the parameters tested, the QRSSTT integral, the STT integral, and the T-wave apex amplitude applied in single, selected leads, showed to be the optimal variables in the detection of prior MI. The areas under the receiver operating characteristic (AUC) curves were 89% for each, and detection was equal in old and recent MI (AUCs ranging from 87% to 90%), and in QMI and NQMI (AUCs ranging from 88% to 90%) (Tables 11. and 12.).

T apex detected MI optimally in the place of conventional lead V6 (lead 76). The QRSSTT integral detected MI optimally in left lower flank (lead 69) (Figure12.).

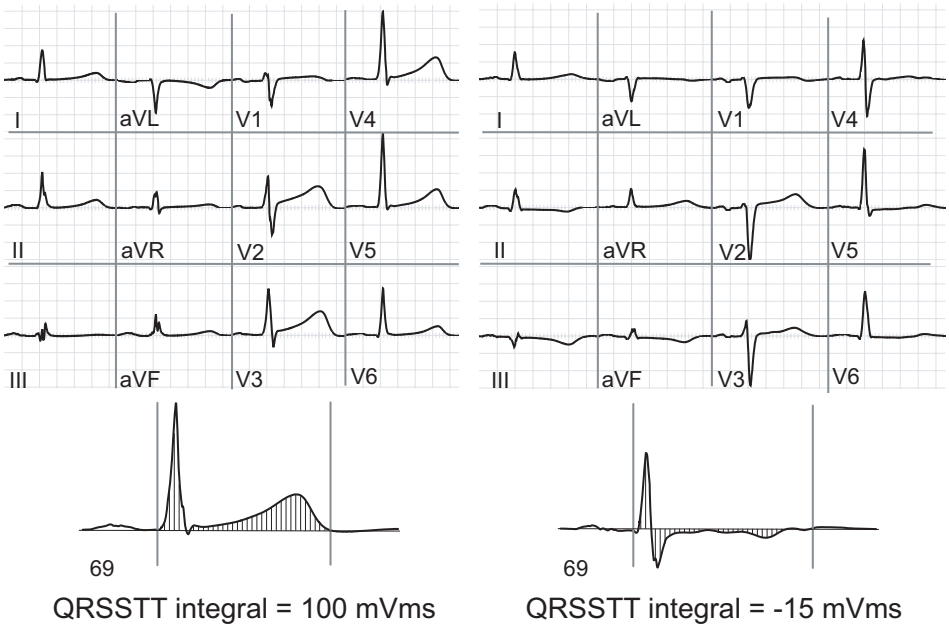

Figure 12 *ECG examples of a healthy control on the left and a patient with a non-Q-wave myocardial infarction (NQMI) on the right. Above are displayed the standard 12-lead ECGs, below are displayed the ECGs recorded in the optimal lead for myocardial infarction detection for the QRSSTT integral. The numerical QRSSTT integral values are shown for the control on the left and for the NQMI patient on the right.*

The group average absolute QRSSTT integral values were predominantly smaller in the MI group than in the control group.

With matched sensitivity to the Minnesota code of 68%, the specificity for the optimal lead for MI detection was 91% for the T apex and 90% for the QRSSTT integral.

The T apex and the QRSSTT integral produced equal AUCs in the old and recent MI groups. In the old MI group the absolute QRSSTT integral values were consistently smaller than in the recent MI group.

The T apex, the QRSSTT integral, and the STT integral made no distinction between the QMI and NQMI groups (AUCs of 58 - 60%, p = ns for all).

Table 11. *AUC of optimal lead for parameters in detection of prior MI (IV)*

Parameter	AUC (CI) of optimal lead (%)	Optimal lead location
T-apex amplitude	89 (85-94)	76
QRSSTT integral	89 (85-93)	69
STT integral	89 (84-93)	76
QRS integral	85 (79-90)	41

AUC=area under receiver operating characteristic curve, CI=95% confidence interval, MI=myocardial infarction

Table 12. *AUC of optimal lead for parameters of MI detection in MI subgroups (IV)*

Parameter	MI	AUC (CI) (%)	Optimal lead location
T-apex amplitude	Old MI	90 (85-94)	76
	Recent MI	87 (80-95)	72
	QMI	90 (85-94)	76
	NQMI	89 (82-96)	76
QRSSTT integral	Old MI	88 (83-93)	62
	Recent MI	90 (85-95)	63
	QMI	90 (85-95)	62
	NQMI	88 (81-94)	69

AUC=area under receiver operating characteristic curve, CI=95% confidence interval, MI=myocardial infarction

In the subgroup analysis according to MI location the optimal leads for detecting solitary MI in all three locations, anterior, inferoposterior, and apical, yielded AUCs of greater than 90% ($p<0.001$ for all) for the QRSSTT integral, T-wave apex amplitude, and the STT integral (Table 13.).

The QRSSTT integral distinguished between solitary anterior and solitary inferoposterior MI optimally on left shoulder (AUC of 86%, CI 78-94%). The T-apex amplitude distinguished between the subgroups optimally on left lower back (AUC of 91%, CI 81-97%).

In the multiple MI location subgroups the QRSSTT integral and the T-apex amplitude outperformed the Minnesota code in every location (Table 14.).

Table 13. *Areas under receiver operating characteristic curves (AUC) for detection of solitary prior myocardial infarction (MI) by use of the optimal leads. CI =95% confidence interval (V).*

	AUC (CI) of the optimal lead (%)	The optimal lead location
MI location	QRSSTT integral	
Anterior	93 (87-99)	Above V_4 and V_5
Inferoposterior	92 (88-97)	Lower left flank
Apical	95 (88-100)	Above V_4 and V_5
	T-apex amplitude	
Anterior	92 (85-98)	Above V_5
Inferoposterior	95 (90-99)	Below V_6
Apical	91 (81-100)	Above V_4 and V_5

Table 14. *Sensitivity and specificity of quantitative body surface potential mapping (BSPM) variables and Minnesota code in detecting prior myocardial infarction (MI) with respect to MI location. Top row shows the sensitivities and specificities of Minnesota code. In the rows below are presented the sensitivities and specificities of the BSPM parameters calculated by a cross validation method (V).*

	Anterior MI		Inferoposterior MI		Lateral MI	
	Sensitivity	Specificity	Sensitivity	Specificity	Sensitivity	Specificity
Minnesota code	53%	59%	35%	91%	20%	95%
QRSSTT integral	73%	93%	69%	93%	80%	93%
T-apex amplitude	71%	93%	82%	93%	87%	92%

5.1.5 QRSSTT time integral and the T maximum amplitude in evolving ischemic myocardial injury (VI)

The optimal variables for detecting evolving ischemic myocardial injury and insult, as compared to the healthy controls, were the T-apex amplitude with AUC in the optimal lead of 85% ($p<0.001$), and the QT integral with AUC of 85% ($p<0.001$), followed by the STT integral with AUC of 83% ($p<0.001$) (Table 15.). The single-lead QT integral detected evolving myocardial injury with a sensitivity of 90% and specificity of 50%, while the conventional 12-lead ECG ST-segment based criteria showed a sensitivity of 85% and a specificity of 36%. This optimal lead for the QT integral in ischemia detection was located between the standard V4 and V5 (lead 68).

Addition of LVH patients into the control group did not significantly deteriorate the AUC for the QT integral (p=0.484).

The variables were compared with the conventional ST-segment amplitude value. The single-lead ST segment amplitude was inferior to the single-lead QT integral (AUCs of 71% and 85%, respectively, p<0.01) in detecting evolving myocardial ischemic insult and injury. The absolute value of ST-segment amplitude, performed similarly to the ST-segment amplitude.

The QT integral detected ischemia induced by occlusion of any culprit artery better than the ST-segment amplitude. In the optimal lead (68) for ischemia detection for all the patient groups the QT integral produced AUCs of 90%, 80%, and 81% for LAD, RCA, and LCX occlusion, respectively. The optimal leads for ischemia detection for each of the culprit arteries, LAD, RCA, and LCX produced AUCs of 91%, 81%, and 88%, respectively. All these leads lay in the vicinity of each other on the left flank area.

The group average QT integral absolute values were decreased in patients relative to the controls in almost all body surface areas (Figure 13.).

Table 15. *Variables and their optimal locations for detecting myocardial ischemia*

	AUC (CI) % MI vs Controls	AUC (CI) % MI vs Controls and LVH	Optimal lead
T apex amplitude	85 (79-91)	78 (71-84)	71
QT integral	85 (79-91)	82 (76-88)	68
STT integral	83 (77-90)	74 (67-81)	71
ST-segment amplitude	71 (63-79)	70 (63-77)	34
Absolute ST-segment amplitude	72 (64-80)	67 (59-75)	33

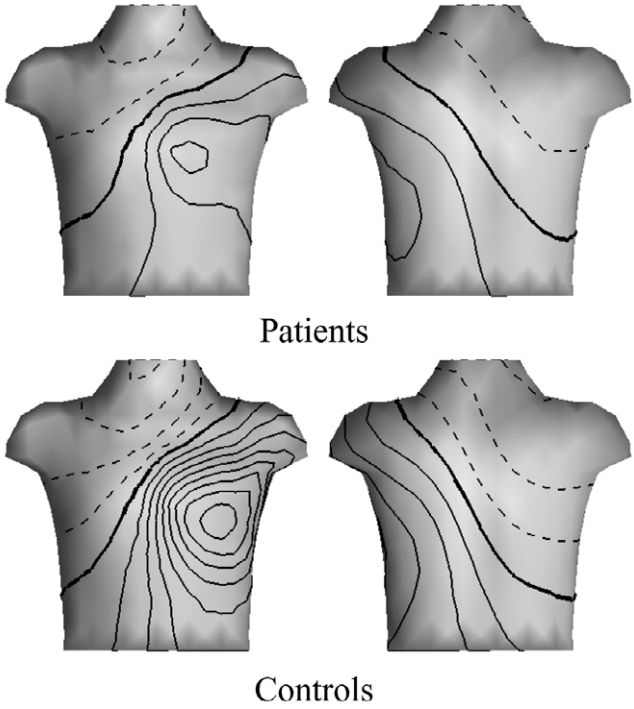

Figure 13 *Group average QT isointegral body surface maps. The thick line represents the zero line, the solid lines positive values, and the dashed lines negative values. Isointegral step is 10 mVms (VI).*

6 DISCUSSION

6.1 Main findings

Continuous, automatically determined variables were equal or superior to the conventionally applied 12-lead ECG descriptive variables in detecting prior MI and evolving myocardial ischemic injury and insult. They were functional assessed in single lead only and outperformed or were equal to the more complex conventional criteria. Moreover, they were efficacious over wide thoracic regions and thus indifferent to slight lead displacements.

Of the tested variables the optimal ones proved to be the QT integral (i.e. the QRSSTT integral), the T-maximum amplitude, and the STT integral, both in prior MI and in the evolving ischemic injury and insult. These repolarization variables, especially the QT integral, were equally effective in MI detection irrespective of time elapsed from prior MI, the Q-waves status, or MI location. Even during the evolving ischemic phase the detection of ischemia by the QT integral was equal irrespective of the culprit artery. The performance of the QT integral was not hampered by underlying LVH. We emphasized the QT integral at the expense of the equally good T-maximum amplitude, because the height of the apex of the T wave is partly determined by the angle at which it is recorded with respect to the transmural axis (Yan and Antzelevitch 1998), and we therefore deemed the T-apex amplitude unreliable.

Whereas the repolarization variables detected MI and evolving ischemic injury and insult irrespective of its determinants, the depolarization variables appeared to be more related to the Q-wave status, size, and location of prior MI. The different time segments of depolarization detected prior MI differently according to its location and the initial segments also correlated with MI size.

6.2 MI and the ventricular gradient

Both prior MI and evolving ischemic injury and insult decreased the absolute QRSSTT integral values over nearly the whole thoracic surface. This decrease may partially be attributable to decrease in electrically functional myocardium, partially to the inversion of the polarity of the QRS and STT induced by MI and evolving ischemic injury. The absolute QRSSTT integral values further decreased in the old MI as compared to the recent MI, despite equal LVEF. Thus, the absolute QRSSTT integral appears to diminish with time elapsing from MI. This probably represents a later process of LV remodelling, since the variable weakly correlated with the age of recent MI. The QRSSTT integral parameter as an indicator of MI, thus, seems resistant to normalisation over time.

The positive spatial correlation of the STT integral to the QRS integral in healthy heart was reversed both in old MI and in evolving ischemic injury. Of importance is that the negative correlation of QRS and STT integrals was strong also in NQMI patients. This inversion provides explanation to the efficiency of the QRSSTT integral in detecting MI: as the QT integral parameter is the sum of the QRS and STT integrals, inverse polarity produces QRSSTT integral values approaching zero, whereas concordant polarity produces values departing from zero. The QRSSTT value map distribution was similar with regard to polarity and zero line in the patients and the controls (Figure 9.). The optimal map areas for the QRSSTT integral variable appeared to have a relatively steep gradient for the QRSSTT integral in the controls. This gave contrast to the low QRSSTT integral values of the patients in the same area.

The distinction between the isocontour maps of the MI patients and the controls was more pronounced in the STT integral than in the QRS integral, reflecting the better ability of the STT variables, in quantitative analysis, to detect MI. T-wave form and amplitude are principally the results of transmural voltage gradients (Franz et al.1987, Yan and Antzelevitch 1998). MIs may disrupt the M cell region (Yan and Antzelevitch 1998) and affect the transmural gradient thereby inducing surface-ECG alterations in disproportion to the infarct size. Our study demonstrates this by showing the ability of the variables covering the repolarisation phase to detect MI regardless of Q-wave status and MI size.

The optimal locations for the QT integral variable lay in the region of the steepest voltage gradient, for both depolarization and repolarization. Supposedly this should have influenced the reliability of the recording due to the risk of slight lead displacement. The QT integral, however, was relatively indifferent to such displacements, owing to the inversion of the QRS and STT integral maps. Should the displacement affect the QRS integral value, it simultaneously alters the STT integral value of opposite polarity, resulting in zero net effect in the pathologic QT integral. The situation in the healthy is somewhat different, however. In the area of the steepest voltage gradient, displacement induced change in the QRS integral value may result in inconsistent alterations in the STT integral, depending on the direction of displacement. This is reflected by the greater dispersion of the QRS and STT integral spatial correlation scatter plots in the controls as compared to the patients. With a single lead this may result in increased sensitivity, but reduced specificity closer to the steep gradient area, and vice versa further away. Therefore, it would probably be practical to record with two leads: one at the steep gradient area, and one at distance from it, for example the right shoulder, to allow for optimal specificity.

6.3 Performance of the ECG variables according to MI location

The repolarisation variables, in addition to the early depolarisation variables, were capable of detecting prior MI irrespective of MI location and exceeded the qualitative Minnesota code in detecting prior MI in every infarct location despite the advantage given to the

Minnesota code by the exclusion of controls with Q-waves (II, IV, V). Moreover, they were able to distinguish between the MI locations (V).

The optimal chest area for detecting prior MI in every MI location by repolarisation variables was the left flank, outside the standard 12 leads, with the exception of the STT integral in lateral MI on right upper chest. Anterior MI appeared optimally above the standard lateral leads and inferoposterior MI below the standard lateral leads (V).

The temporal analysis of the depolarization wave exhibited variation according to MI location. Anterior MI was best detected during the early part of the QRS complex, as expected. For the lateral MI the first half of the QRS complex was the most informative. The inferior and posterior MIs were best detected during the mid QRS, with MI detection for inferior MI peaking slightly earlier than for posterior MI. The apical MI was best detected during late QRS (I). This timing of best performance within the QRS complex is in agreement with the known sequence of distribution of the depolarization wave in the heart except for the early detection of lateral and late detection of apical MI (Surawitcz 1995b).

In our patients anterior MI manifested as negative DI values over most of the anterior chest during all sextiles. Thus, the MI group had decreased time integral values anteriorly due to the loss of myocardium in the anterior LV wall. Inferior and posterior MI manifested as negative DI values over the anterior lower thorax during the mid QRS. These observations are in agreement with previous findings of anterior MI presenting as negative values over the anterior thorax and inferior MI as negative values over the inferior torso during depolarization (Montague et al.1986a).

6.4 Contribution to previous studies

Whereas the conventional criteria and coding systems for prior MI mainly rely on the initial QRS deflection, in these studies the best diagnostic variables were based on repolarization and the whole electrical systolic cycle. The 1st quartile of QRS integral conventionally exploited in prior MI diagnostics showed inferior diagnostic capability.
The repolarisation parameters detected prior QMI and NQMI infarctions equally and made no distinction between the two. The depolarisation parameters, however, detected QMI slightly better than NQMI and marginally distinguished QMI from NQMI. The best depolarisation parameter, the 2nd QRS quartile integral, correlated with LVEF ($r=0.42$, $p<0.001$). This is in concordance with a correlation of 0.44 found between QRS scoring and anatomical size of multiple MI (Sevilla et al. 1992) and the observed relation of Q-wave with larger MI size (Moon et al. 2004).

Our findings of the 1st and the 2nd QRS quartile being the best of the depolarization wave in detecting MI, and with the last two sextiles being non-informative is well in concordance with the findings of Franz et al that the endocardial activation times (AT) fitted within the first third of the QRS deflection and the epicardial ATs within the first two thirds of the QRS (Franz et al. 1987).

The repolarisation variables detected old and recent MI equally well, and with elapsing time the repolarisation abnormalities increased, in contrast to greater regression of ST-T-wave changes than Q waves reported earlier (Cox 1967, Kaplan and Berkson 1964). The repolarization variables, thus, represent a time-resistant method of MI detection.

The ventricular gradient, defined as the time integral of the lead voltage over the systolic electrical cardiac cycle, i.e. the QRSSTT integral or the QT integral, was introduced more than 70 years ago (Wilson et al. 1934, Geselowitz 1983). Yet, it has only incidentally been studied in conjunction with myocardial infarction or ischemia and no clear cut conclusions of its usability in this purpose exist (Burgess et al. 1978, Claydon et al. 1991, Ikeno et al. 1995, Nishiyama et al. 1993, Adachi et al. 1991, Nash et al. 2003). In a study on porcine hearts the occlusion of a coronary artery caused increase in epicardial and body surface QRST integral values (Nash et al. 2003). In our study, the QRSSTT integral values were consistently decreased in MI patients as compared to controls, both in the chronic phase and evolving ischemic injury and insult. Our findings would imply greater ventricular gradient in healthy than in diseased hearts, and additionally, in normal hearts, greater spatial dispersion of the ventricular gradient. Our studies confirmed previous observations that the QRS and STT integrals are positively correlated in healthy controls (Montague et al. 1981). Thus, the polarity and magnitude of the depolarization and repolarization of the ventricles are mainly concordant in healthy subjects.

The spatial QRS-T angle, akin to the ventricular gradient, is a strong and independent predictor of cardiac mortality, sudden death, and total mortality in general population of over 55 years of age (Kardys et al. 2003). As the QT integral reflects the same phenomenon, this predicting ability of the QRS-T angle may partly be due to unrecognized MIs.

In our study the QT integral identified evolving ischemic injury and insult. While the QRS-T angle in the setting of acute chest pain is associated with increased long-term mortality risk, it interestingly, has no relation to the final cardiac diagnosis (de Torbal et al. 2004). The spatial QRS-T angle is, however, able to identify patency of the infarct related artery after thrombolysis (Dilaveris et al. 2005).

The ability of the variables covering the repolarisation phase to detect MI regardless of Q-wave status and MI size may reflect disruption the M cell region by small MIs affecting the transmural gradient and thereby altering the surface ECG in disproportion to the infarct size (Yan and Antzelewitch 1998). It is therefore understandable that pathological Q-waves and ST-T abnormalities are found more frequently in non-transmural than transmural MI, (Sievers et al. 2004) and that the prediction of transmurality by the Q-wave status has been futile (Moon et al. 2004).

The repolarization variables as well as the early depolarization variables were functional when recorded in a single lead, and attained or even exceeded the conventional methods for MI detection (IV, V, VI). The various established coding systems exploit information derived from multiple leads for the diagnosis of prior MI, as do studies that demonstrate the prognostic ability of the QRS-T angle or its equivalents (Kardys et al. 2003, de Torbal

et al. 2004, Zabel et al. 2000). Furthermore, the repolarization variables recorded in a single lead only were useful also in evolving ischemic injury (VI). Previously in an acute state of myocardial ischemia and monitoring situations multiple lead recordings have proved superior to fewer lead-combinations (Menown et al. 2001, Klootwijk et al. 1997).

The analysis of time integrals is likely to be a relatively reproducible and stable method as opposed to instantaneous potential values within the electrical cardiac cycle (Kornreich et al. 1985, Kornreich et al. 1986, Kornreich et al. 1991). The individual anatomy and deviation in lead placement causing temporal variation of potentials is probably less likely to introduce bias in the time integral analysis.

6.5 Study limitations

In all the substudies patients with bundle branch block, atrial fibrillation, and patients with pacemaker or using drugs affecting repolarization were excluded. These patients compose a substantial proportion of patients seeking medical aid for chest pain, both acutely and electively. The recruitment of patients into all of the substudies was profoundly reliant on deviant ECG findings among the hospitalized patients. The patients with normal or ambiguous 12-lead ECGs are, therefore, underrepresented. In the final substudy (VI) the BSPM was acquired in a subacute phase of evolving ischemic injury and insult, when most of the conventional 12-lead ECG signs of acute ischemia had subsided. The conclusions are not, therefore, applicable to the hyperacute state of ischemia, but warrant further research. Moreover, further research is also required to identify a cut-off value, not proposed in these studies, for the identification of MI or evolving ischemic injury.

6.6 Clinical implications

Selection from the abundant information gained in BSPM studies will allow introduction of simpler and more accurate lead-combinations for the detection of prior MI and acute ischemia and AMI in the future. The variables are applicable also to standard 12-lead ECG and thus would allow re-analysis of pre-existing digital ECG databases. The single-lead recording and analysis offers potential for monitoring in acute ischemic situations.

Time segment analysis of the depolarization wave offers potential to improve the detection and localization of prior MI. Time segmentation can localize subendocardial MIs and NQMI, which is impossible with the conventional ECG methods.

The QT integral and the spatial inversion of QRS and STT integrals might hold potential for risk stratification in post-MI patients, as does the angle between depolarization and repolarization wavefronts (Zabel et al. 2000). Future studies are warranted to see whether the QT integral has prognostic value for adverse cardiac events and survival.

7 CONCLUSIONS

We have found a variable, the QT integral, detectable in a single lead, describing the phenomenon of divergence of the depolarization and repolarization wavefronts, and being able to detect prior MI and acutely evolving myocardial injury more effectively than the conventional ECG markers and possibly offering potential for risk stratification.

The automatically determined quantitative variables were capable of detecting prior MI irrespective of MI location. In particular the repolarisation variables, in addition to the early depolarisation variables, were optimal in this function. Furthermore, the quantitative variables exceeded the qualitative Minnesota code in detecting prior MI in different infarct locations, and in detecting MI also in the absence of Q-waves. Moreover, the studied variables, repolarisation and early depolarisation variables, were able to distinguish between the MI locations. Thus the presently studied automatically determined quantitative, single lead parameters performed comparably or superior to the more complex MI classification systems.

Our studies suggest that ventricular depolarisation is more affected by the Q-wave status and the size of MI, whereas repolarisation appears to depend less on the infarct size and Q-wave status.

In conclusion, the optimal quantitative variable for the detection of prior MI and evolving myocardial injury proved to be the QT integral. As an improvement to the traditional ECG diagnostis of ischemia and infarction, it appeared time-resistant in prior MI and independent of location in myocardium in both previous and evolving injury. Furthermore, it appeared superior to the conventional ECG interpretation methods. Most importantly the QT integral was efficient when recorded in a single lead, the location of which was slightly deviant from the standard 12-lead locations, making it potentially applicable for screening purposes and ischemia monitoring.

ACKNOWLEDGEMENTS

This study was carried out from 2001 to 2007 at the Cardiovascular Laboratory of the Division of Cardiology, Department of Medicine, and the BioMag Laboratory of the Helsinki University Central Hospital. Studies I-V were carried out on previously collected patient data. Study VI is part of the ISKE-project, a collaborative project of the Division of Cardiology of the Helsinki University Central Hospital and the Laboratory of Biomedical Engineering at the Helsinki University of Technology. I am very grateful to Professor Markku S. Nieminen, M.D., Ph.D., Head of the Division of Cardiology, for placing its excellent research facilities at my disposal, for making the ISKE-project possible, for introducing me to the supervisor of this thesis, and for supporting me in my endeavors throughout the years. I also wish to thank Professor Markku Kupari, M.D., Ph.D., Head of the Cardiovascular Laboratory for the laboratory research facilites and for his positive attitude toward my work.

I am indebted to Professor Toivo Katila, D.Sc. (Tech.), the former Head of the Laboratory of Biomedical Engineering and the former leader of the interdisciplinary graduate school "Functional Research in Medicine" and to his successor Professor Risto Ilmoniemi, D.Sc. (Tech.), for providing me with excellent research facilities at the Laboratory of Biomedical Engineering at the Helsinki University of Technology, and for supporting the ISKE-project. I wish to extend my gratitude to Docent Juha Montonen, D.Sc. (Tech.), Head of the BioMag Laboratory, for the unique research facilities in the BioMag Laboratory, essential for this study.

I have had the privilege to work under the guidance of a distinguished clinical electrophysiologist and scientist, Docent Lauri Toivonen, M.D., Ph.D., whose ideas have been the source of inspiration for these studies. He has continuously provided me with his expert scientific advice and friendly support, but encouragingly left room for my own thoughts and ideas. Under his supervision I have had the chance to work at my own pace, yet always with a possibility for counselling when needed.

I also wish to extend my deepest gratitude to my other supervisor, Docent Markku Mäkijärvi M.D., Ph.D., for his encouragement and continuous positive attitude toward my work, for introducing me to numerous highly acknowledged scientists from all over the world, and for providing aid in my practical problems as well.

I extend my gratitude to Professor Mikael Dellborg, M.D., Ph.D, and Professor Jari Hyttinen, D.Sc.(Tech.), the reviewers of this thesis, for their constructive criticism and valuable advice concerning the final manuscript.

I wish to thank all my research collaborators for their invaluable contribution to this thesis. I am immensely grateful to Helena Hänninen, M.D. Ph.D., who has introduced me into the world of body surface potential mapping (BSPM), kindly provided me with study material, both in terms of literature and patients, and taught me the basics of computed ECG analysis. I am deeply indebted to Heikki Väänänen, M.Sc. (Tech.), the creator of the tool for the analysis of the ECG recordings, for his guidance in the use of this tool, for coordinating the ISKE-project, for aid in scientific and technical problems, as well as for helpful comments on my manuscripts. I truly appreciate the time and effort he has offered to this project. I owe my sincerest thanks to Mats Lindholm, B.Sc., who has effectively

operated the BSPM recording device and software, and coordinated the patient data within the laboratory. My sincere gratitude is expressed to Matti Stenroos, M.Sc. (Tech.), who has provided our research group with tools for statistical and illustratory work. I owe my thanks to Docent Jukka Nenonen, D.Sc. (Tech.), whose expertise was essential for this study. I gratefully acknowledge the enthusiastic and competent work of Minna Kylmälä, M.D., who has continued the recruiting and investigating of the patients for the ISKE-project and created new, innovative study protocols. I gratefully acknowledge the aid and support of Juhani Dabek, B.Sc. (Tech.), Teijo Konttila, B.Sc. (Tech.), and Milla Karvonen, M.Sc. (Tech.). I wish to extend my gratitude to Ilkka Tierala, M.D., a fellow researcher and outstanding clinician, highly appreciated amongst the patients, for his aid in the recruitment of the study patients and for his clinical and scientific advice. I express my sincere gratitude to Lasse Oikarinen, M.D., Ph.D., who has always had the patience to answer my questions, for his friendly encouragement. I owe my thanks to Petri Korhonen, M.D., Ph.D., and Terhi Husa, M.D., for providing me with study subjects and for scientific advice. I am deeply indebted to Kirsi Lauerma, M.D., Ph.D., who performed and interpreted cardiac magnetic resonance (CE-CMR) investigations for our study patients and Miia Holmström M.D., Ph.D., who interpreted the CE-CMR images and offered her help and expertise. I highly appreciate the scientifically inspiring conversations, both in person and by e-mail, with all my collaborators. I am truly grateful to Hanna Ranne, R.N. and Suvi Heikkilä, R.N., for their invaluable assistance in patient registrations, and Leena Lajunen for the excellent library services. I wish to thank my dear godmother, Docent Ritva Leppihalme (Department of English, Helsinki University) for linguistic advice and for her support.

I want to express my appreciation to the patients, and also volunteers, who have participated in these studies. Their positive attitude toward clinical research has made this study possible. I also wish to thank the personnel of the Cardiovascular laboratory and the Emergency Units in Meilahti Hospital for their helpful and tolerant attitude toward research work.

I wish to express my gratitude to my dear friend Arja Muhonen, D.D.S., Ph.D., who has provided me with invaluable support and understanding of all of the problems faced by a mother of three who is a researcher. I am also grateful to my friend and colleague Marjo Tamminen, M.D., Ph.D. for her priceless advice and support, as a friend and colleague in clinic and in science.

I owe my deepest gratitude to my parents, Varpu and Matti, for their love and encouragement in my life. Their loving care of my sons during these years has been invaluable.

Finally, I want to express my sincerest gratitude to Mika, my loving husband, for his encouragement towards my work during these years, and most importantly, for being an excellent father to our three beautiful sons. I owe my deepest gratitude and love to my sons, Tuure, Reko, and Lalli, who have donated what is most valuable to them, the time and attention of their mother. You are the essence of my life.

This work was financially supported by the Finnish Foundation for Cardiovascular Research, the Aarne Koskelo Foundation, the Finnish Medical Society Duodecim, the

Paulo Foundation, the Aarne and Raili Turunen Foundation, and the Finnish Funding Agency for Technology and Innovation (TEKES), which I gratefully acknowledge.

Helsinki, August 2007

Paula Vesterinen

.

REFERENCES

Abildskov JA, Burgess MJ, Millar K, Wyatt R, Baule G. The primary T wave-a new electrocardiographic waveform. Am Heart J; 1971; 81:242-249.

Abildskov JA, Evans AK, Lux RL, Burgess MJ. Direct evidence relating QRST deflection area and ventricular recovery properties. Circulation 1979;60 (Suppl II):II-110.

Acar B. Yi G. Hnatkova K. Malik M. Spatial, temporal and wavefront direction characteristics of 12-lead T-wave morphology. Med Biol Eng Comput 1999; 37(5):574-84.

Ackaoui A, Nadeau R, Sestier F, Savard P, Primeau R, Lemieux R, Descary M. Myocardial infarction diagnosis with body surface potential mapping, electrocardiography, vectorcardiography and thallium-201 scintigraphy: a correlative study with left ventriculography. Clin Invest Med 1985:8(1): 68-77.

Adachi M, Hayashi H, Hirai M, Tomita Y, Ichihara Y, Suzuki A, Kondo K, Inagaki H, Saito H. Usefulness of QRST time-integral values of 12-lead electrocardiograms in diagnosing healed myocardial infarction complicated by left bundle branch block. Am J Cardiol 1991;68:1417-23.

Adams J, Trent R, Rawles J. Earliest electrocardiographic evidence of myocardial infarction: Implications for thrombolytic treatment. British Medical Journal 1993; 307:409-413.

Ambroggi L, Bertoni T, Rabbia C, Landolina M. Body surface potential maps in old inferior myocardial infarction. Assessment of diagnostic criteria. J Electrocardiol 1986:19 (3): 225-234.

Andersen A, Dobkin J, Maynard C, Myers R, Wagner GS, Warner RA, Selvester RHS. Validation of advanced ECG diagnostic software for the detection of prior myocardial infarction by using nuclear cardiac imaging. J Electrocardiol 2001; 34 (Suppl):243-248.

Andersen A, Gasperina MD, Myers R, Wagner GS, Warner RA, Selvester RHS. An improved automated ECG algorithm for detecting acute and prior myocardial infarction. J Electrocardiol 2002;35(Suppl):105-110.

Antoni H. Function of the heart. In Human physiology. Schmidt RF, Thews G Eds. 2nd edition, Springer-Verlag 1989, Berlin, Heidelberg. 439-451.

Antzelevitch C, Shimizu W, Yan G-X, Sicouri S, Weissenburger J, Nesterenko V, Burashnikov A, Di Diego J, Saffitz J, Thomas GP. The M Cell: Its contribution to the ECG and to normal and abnormal electrical function of the heart. J Cardiovasc Electrophysiol 1999; 10:1124-1152.

Antzelevitch C. Tpeak-Tend interval as an index of transmural dispersion of repolarization. Eur J Clin Invest 2001; 31:555-557.

Aude YW, Mehta JL. Do we need continuous ECG monitoring in patients transferred for primary angioplasty? Eur Heart J 2006; 27:249-250.

Barbagelata, A. Califf, R M. Sgarbossa, E B. Goodman, S G. Stebbins, A L. Granger, C B. Suarez, L D. Borruel, M. Gates, K. Starr, S. Wagner, G S. Thrombolysis and Q wave versus non-Q wave first acute myocardial infarction: a GUSTO-I substudy. Global Utilization of Streptokinase and Tissue Plasminogen Activator for Occluded Arteries Investigators. J Am Coll Cardiol 1997; 29:770-7.

Batchvarov V. Dilaveris P. Farbom P. Ghuran A. Acar B. Hnatkova K. Camm AJ. Malik M. New descriptors of homogeneity of the propagation of ventricular repolarization. Pacing & Clinical Electrophysiology 2000;23(11 Pt 2):1968-72.

Batchvarov V. Hnatkova K. Ghuran A. Poloniecki J. Camm AJ. Malik M. Ventricular gradient as a risk factor in survivors of acute myocardial infarction. Pacing & Clinical Electrophysiology 2003;26(1 Pt 2):373-6.

Batchvarov V. Kaski JC. Parchure N. Dilaveris P. Brown S. Ghuran A. Farbom P. Hnatkova K. Camm AJ. Malik M. Comparison between ventricular gradient and a new descriptor of the wavefront direction of ventricular activation and recovery. Clinical Cardiology 2002;25(5):230-6,.

Batchvarov VN, Hnatkova K, Poloniecki J, Camm AJ. Malik M. Prognostic value of heterogeneity of ventricular repolarization in survivors of acute myocardial infarction. Clinical Cardiology 2004;27(11):653-9.

Battler A. European Heart Survey of Acute Coronary Syndromes. Eur Heart J. 2002; 23:1190-201.

Bergovec M, Prpic H, Zigman M, Vukosavic D, Birtic K, Mihatov S, Franceschi D, Baric L. Regression of ECG signs of myocardial infarction related to infarct size and left ventricular function. J Electrocardiol 1993;26:1-8.

Bertrand ME, Simoons ML, Fox KAA, Wallentin LC, Hamm CW, McFadden E, De Feyter PJ, Specchia G, Ruzyllo W. Management of acute coronary syndromes in patients presenting without persistent ST-segment elevation. The Task Force on the Management of Acute Coronary Syndromes of the European Society of Cardiology. Eur Heart J 2002; 23:1809-1840.

Braunwald E, Cannon CP. Non-Q wave and ST segment depression myocardial infarction: Is there a role for thrombolytic therapy? J Am Coll Cardiol 1996; 27:1333-1334.

Burgess MJ, Lux RL, Wyatt RF, Abildskov JA. The relation of localized myocardial warming to changes in cardiac surface electrograms in dogs. Circulation Research 1978;43:899-907.

Cahyadi YH, Murakami E, Takekoshi N, Matsui S, Fujita S, Tsugawa H, Miyamoto M, Maeda T, Miyagawa S. Body surface potential mapping in anterior myocardial

infarction—a longitudinal study in acute, convalescent and chronic phases. Jpn Circ J 1989; 53:206-12.

Carley S, Mackway-Jones K, Jenkins M, Darlington E, Fath-Ordoubadi F, Curzen N. A novel method for the detection of transient myocardial ischemia using body surface electrocardiac mapping. Int J Cardiol 2004; 95:75-81.

Carley S. Beyond the 12 lead: review of the use of additional leads for the early electrocardiographic diagnosis of acute myocardial infarction. Emerg Med 2003; 15:143-54.

Carley SD, Jenkins M, Jones KM. Body surface mapping versus the standard 12-lead ECG in the detection of myocardial infarction amongst Emergency Department patients: a Bayesian approach. Resuscitation 2005; 64:309-14.

Claydon FJ, Ingram LA, Mirvis DM. Effects of myocardial infarction on cardiac electrical field properties using a numerical expansion technique. J Electrocardiol 1991;24:371-377.

Cox CJB. Return to normal of the electrocardiogram after myocardial infarction. Lancet 1967;X:1194-1197.

De Ambroggi L, Bertoni T, Rabbia C, Landolina M. Body surface potential maps in old inferior myocardial infarction: assessment of diagnostic criteria. J Electrocardiol 1986; 19:225-.

De Torbal A, Boersma E, Kors JA, van Herpen G, Deckers JW, van der Kuip DAM, Stricker BH, Hofman A, Witteman JCM. Incidence of recognized and unrecognized myocardial infarction in men and women aged 55 and older: the Rotterdam Study. Eur Heart J 2006; 27:729-736.

De Torbal A, Kors JA, van Herpen G, Meij S, Nelwan S, Simoons ML, Boersma E. The electrical T-axis and the spatial QRS-T angel are independent predictors of long-term mortality in patients admitted with acute ischemic chest pain. Cardiology 2004;101:199-207.

Dilaveris P, Anastasopoulos A, Androulakis A, Theoharis A, Zumerle B, Tzannetis G, Kallikazaros I, Stefanadis C. Effects of thrombolysis on vectorcardiographic indices of ventricular repolarization: correlation with ST-segment resolution. J Electrocardiol 2005; 38:347-53.

Dilaveris P, Gialafos E, Pantazis A, Synetos A, Triposkiadis F, Stamatelopuolos S, Gialafos J. Spatial aspects of ventricular repolarization in postinfarction patients. Pacing & Clinical Electrophysiology 2001; 24:157-65.

Dower GE, Yakush A, Nazzal SB, Jutzy RV, Ruiz CE. Deriving the 12-lead electrocardiogram from four (EASI) electrodes. J Electrocardiol 1988; 21(Suppl):182-7.

Effects of tissue plasminogen activator and a comparison of early invasive and conservative strategies in unstable angina and non-Q-wave myocardial infarction. Results of the TIMI IIIB Trial. Thrombolysis in Myocardial Ischemia. Circulation 1994;89:1545-56.

Engblom H, Wagner GS, Setser RM, Selvester RH, Billgren T, Kasper JM, Maynard C, Pahlm O, Arheden H, White RD. Quantitative clinical assessment of chronic anterior myocardial infarction with delayed enhancement magnetic resonance imaging and QRS scoring. Am Heart J 2003; 146:359-66.

Engblom H, Wagner GS, Setser RM, Selvester RH, Billgren T, Kasper JM, Maynard C, Pahlm O, Arheden H, White RD. Quantitative clinical assessment of chronic anterior myocardial infarction with delayed enhancement magnetic resonance imaging and QRS scoring. Am Heart J 2003;146:359-66.

Erhardt L, Herlitz J, Bossaert L, Halinen M, Keltai M, Koster R, Markassa C, Quinn T, Van Weert H. Task force on the management of chest pain. Eur Heart J 2002; 23:1153-1176.

Farr BR, Vondenbusch B, Silny J, Rau G, Effert S. Localization of significant coronary arterial narrowings using body surface potential mapping during exercise stress testing. Am J Cardiol 1987;59:528-530.

Feldman LJ, Himbert D, Juliard JM, Karrillon GJ, Benamer H, Aubry P, Boudvillain O, Seknadji P, Faraggi M, Steg G. Reperfusion syndrome: Relationship of coronary blood flow reserve to left ventricular function and infarct size. J Am Coll Cardiol 200; 35:1162-9.

Flowers NC, Horan LG. Body surface potential mapping. In: Cardiac electrophysiology, Zipes & Jalife, 2nd edition 1995:1049-1055.

Fozzard HA, Makielski JC. The electrophysiology of acute myocardial ischemia. Ann Rev Med 1985;36:275-84.

Franz MR, Bargheer K, Costard-Jäckle A, Miller DG, Lichtlen PR. Human ventricular repolarization and T wave genesis. Progress in cardiovascular diseases 1991;33:369-384.

Franz MR, Bargheer K, Rafflenbeul W, Haverich A, Lichtlen PR. Monophasic action potential mapping in human subjects with normal electrocardiograms: direct evidence of the genesis of the T wave. Circulation 1987;75:379-386.

Fuller MS, Dustman TJ, Sharp S, Green LS, Lux R. Optimal lead selection for detection of ST segment shifts. PACE 1996;19:920-928.

Gaudron P, Kugler I, Hu K, Bauer W, Eilles C, Ertl G. Time course of cardiac structural, functional and electrical changes in asymptomatic patients after myocardial infarction: Their inter-relation and prognostic impact. JACC 2001; 38:33-40.

Geselowitz DB. The ventricular gradient revisited: Relation to the area under the action potential. IEEE Transactions on Biomedical Engineering 1983; 30:76-77.

Gibson RS, Beller GA, Gheorghiade M, Nygaard TW, Watson DD, Huey B, Sayre SL, Kaiser DL. The prevalence and clinical significance of residual myocardial ischemia 2 weeks after uncomplicated non-Q wave infarction: a prospective natural history study. Circulation 1986;73:1186-1198.

Goldberg RJ, Gore JM, Alpert JS, Dalen JE. Non-Q wave myocardial infarction: Recent changes in occurrence and prognosis—a community-wide perspective. Am Heart J 1987;113:273-279.

Goldman L, Cook EF, Brand DA, Lee TH, Rouan GW, Weisberg MC, Acampora D, Stasiulewicz C, Walshon J, Terranova G et al. A computer protocol to predict myocardial infarction in emergency department patients with chest pain. N Engl J Med 1988; 318:797-803.

Green LS, Lux RL, Haws CW, Williams RR, Hunt SC, Burgess MJ. Effects of age, sex, and body habitus on QRS and ST-T potential maps of 1100 normal subjects. Circulation 1985,71:244-53.

Green LS, Lux RL, Haws CW. Detection and localization of coronary artery disease with body surface mapping in patients with normal electrocardiograms. Circulation 1987;76:1290-1297.

Griffin B, Timmis AD, Crick JCP, Sowton E. The evolution of myocardial ischemia during percutaneous transluminal coronary angioplasty. Eur Heart J 1987; 8:347-53.

Grijseels EW, Deckers JW, Hoes AW, Hartman JA, Van der Does E, Van Loenen E, Simoons ML. Pre-hospital triage of patients with suspected myocardial infarction. Evaluation of previously developed algorithms and new proposals. Eur Heart J 1995; 16:325-32.

Gruppo Italiano per lo studio della streptochinasi nell'infarcto miocardo (GISSI).Effectiveness of intravenous thrombolytic treatment in acute myocardial infarction. Gruppo Italiano per lo Studio della Streptochinasi nell'Infarto Miocardico (GISSI). Lancet 1986;i:397-402.

Haisty WK, Pahlm O, Wagner NB, Pope JE, Wagner GS. Performance of the automated complete Selvester QRS scoring system in normal subjects and patients with single and multiple myocardial infarctions. J Am Coll Cardiol 1992;19:341-6.

Hanley J, McNeil B: A method of comparing the areas under receiver operating characteristic curves derived from the same cases. Radiology 148:839, 1983.

Harumi K, Burgess MJ, Abildskov JA. A theoretic model of the T wave. Circulation 1966; 34:657-668.

Hauser, A M. Gangadharan, V. Ramos, R G. Gordon, S. Timmis, G C. Sequence of mechanical, electrocardiographic and clinical effects of repeated coronary artery occlusion in human beings: echocardiographic observations during coronary angioplasty. J Am Coll Cardiol 1985;5:193-7.

Hirai M, Ohta T, Kinoshita A, Toyama J, Nagaya J, Yamashita K. Body surface isopotential maps in old anterior myocardial infarction undetectable by 12-lead electrocardiograms. Am Heart J 1984; 108:975-982.

Hlaing T, DiMino T, Kowey PR, Yan GX. ECG repolarization waves :Their genesis and clinical implications. Ann Noninvas Electrocardiol 2005;10:211-223.

Hoffman BF. Electrotonic modulation of the T wave. Am J Cardiol 1982;50:361-362.

Holland RP, Arnsdorf MF. Solid angle theory and the electrocardiogram: Physiologic and quantitative interpretations. Progress in Cardiovascular diseases 1977;19:431-457.

Holland RP, Brooks H. TQ-ST segment mapping: Critical Review and analysis of current concepts. Am J Cardiol 1977;40:10-129.

Horacek BM, Wagner GS. Electrocardiographic ST-segment changes during acute myocardial ischemia. CEPR 2002; 6:196-203.

Horacek BM, Warren JW, Penney CJ, MacLeod RS, Title LM, Gardner MJ, Feldman CL. Optimal electrocardiographic leads for detecting acute myocardial ischemia. J Electrocardiol 2001;34(Suppl):97-111.

Hänninen H, Holmström M, Vesterinen P, Karvonen M, Väänänen H, Oikarinen L, Korhonen P, Mäkijärvi M, Nenonen J, Lauerma K, Katila T, Toivonen L. Magnetocardiographic Assessment of Healed Myocardial Infarction. Ann Noninvas Electro 2006, 11:211-21.

Hänninen H, Takala P, Mäkijärvi M, Korhonen P, Oikarinen L, Simelius K, Nenonen J, Katila T, Toivonen L. ST-segment level and slope in exercise induced myocardial ischemia evaluated with body surface potential mapping. Am J Cardiol 2001; 88:1152-1156.

Ikeno E, Kubota I, Kondo T, Shibata T, Yamaki M, Tomoike H. Diagnostic usefulness of activation-recovery interval for reciprocal ECG changes. Effects of regional myocardial cooling, warming, or cornary occlusion on epicardial electrograms in dogs. J Electrocardiol 1995;28:237-243.

Ishikawa T, Watabe S, Yamada Y, Miyachi K, Sakai Y, Ito A, Sotobata I. New diagnostic evidence on the T wave map indicating involved coronary artery in patients with angina pectoris. Circulation 1988; 77:301-310.

ISIS-2 (second international study of infarct survival) collaborative group. Randomised trial of intravenous streptokinase, oral aspirin, both, or neither among 17 187 cases of suspected acute myocardial infarction: ISIS-2. Lancet 1988; ii: 349-60.

Jernberg T, Lindahl B, Wallentin L. ST-segment monitoring with continuous 12-lead ECG improves early risk stratification in patients with chest pain and ECG nondiagnostic of acute myocardial infarction. J Am Coll Cardiol 1999; 34:1413-09.

Jernberg T, Lindahl B. A combination of troponin T and 12-lead electrocardiography: A valuable tool for early prediction of long-term mortality in patients with chest pain without ST-segment elevation. Am Heart J 2002; 144:804-10.

Jonsdottir LS, Sigfusson N, Sigvaldson H, Thorgeirsson G. Incidence and prevalence of recognized and unrecognized myocardial infarction in women. The Reykjavik Study. Eur Heart J 1998; 19:1011-8.

Kaandorp TA, Bax JJ, Lamb HJ, Viergever EP, Boersma E, Poldermans D, van der Wall EE, de Roos A. Which parameters on magnetic resonance imaging determine Q waves on the electrocardiogram? Am J Cardiol 2005;95:925-9.

Kannel WB, Cupples LA, Gagnon DR. Incidence, precursors and prognosis of unrecognized myocardial infarction. In Kellerman JJ, Braunwald E (eds): Silent myocardial ischemia: A critical appraisal. Adv Cardiol. Basel, Karger, 1990, 37:202-214.

Kaplan BM, Berkson DM. Serial electrocardiograms after myocardial infarction. Annals of Internal Medicine 1964;60:430-435.

Kardys I, Kors JA, van der Meer IM, Hofman A, van der Kuip DAM, Witteman JCM. Spatial QRS-T angle predicts cardiac death in a general population. Eur Heart J 2003; 24:1357-1364.

Kittnar O, Slavicek J, Vavrova M, Barna M, Dohlanova A, Malkova A, Aschermann M, Humhal J, Hradec J, Kral J. Repolarization pattern of body surface potential maps (BSPM) in coronary artery disease. Physiol Res 1993; 42:123-130.

Kleber AG, Janse MJ, van Capelle EJL, Durrer D. Mehcanism and time course of ST and QT segment changes during acute regional myocardial ischemia in the pig heart determined by extracellular and intracellular recordings. Circ Res 1978; 42:603-.

Klootwijk P, Meij S, Melkert R, Lenderink T, Simoons M. Reduction of recurrent ischemia with abciximab during continuous ECG-ischemia monitoring in patients with unstable angina refractory to standard treatment (CAPTURE). Circulation 1998; 98:1358-64.

Klootwijk P, Meij S, von Es GA, Muller EJ, Umans V, Lenderink T, Simoons ML . Comparison of usefulness of computer assisted continuous 48-h 3-lead with 12-lead ECG ischemia monitoring for detection and quantization of ischaemia in patients with unstable angina. Eur Heart J 1997; 18:931-940.

Korhonen P, Husa T, Tierala I, Väänänen H, Mäkijärvi M, Katila T, Toivonen L. Increased intra-QRS fragmentation in magnetocardiography as a predictor of arrhyhtmic events and mortality in patients with cardiac dysfunction after myocardial infarction. J Cardiovasc Electrophysiol 2006;17:1-6.

Korhonen P, Tierala I, Simelius K, Väänänen H, Mäkijärvi M, Nenonen J, Katila T, Toivonen L. Late QRS activity in signal-averaged magnetocardiography, body surface potential mapping, and orthogonal ECG in postinfarction ventricular tachycardia patients. Ann Noninvasive Electrocardiol 2002;7:389-98.

Kornreich F, Montague T, Rautaharju P. Body surface potential mapping of ST segment changes in acute myocardial infarction. Implications for ECG enrollment criteria for thrombolytic therapy. Circulation 1993:87(3): 1040-1042.

Kornreich F, Montague TJ, Rautaharju P. Identification of first acute Q wave and non-Q wave myocardial infarction by multivariate analysis of body surface potential maps. Circulation 1991:84: 2442-2453.

Kornreich F, Montague TJ, Rautaharju PM, Block P, Warren JW, Horacek MB. Identification of best electrocardiographic leads for diagnosing anterior and inferior myocardial infarction by statistical analysis of body surface potential maps. Am J Cardiol 1986;58:863-871.

Kornreich F, Rautaharju PM, Warren J, Montague TJ, Horacek M. Identification of best electrocardiographic leads for diagnosing myocardial infarction by statistical analysis of body surface potential maps. Am J Cardiol 1985;56:852-856.

Kornreich F, Selvester RH, Montague TJ, Rautaharju PM, Saetre HA, Ahmad J. Discriminant analysis of the standard 12-lead ECG for diagnosing non-Q wave myocardial infarction. J Electrocardiol 1992;24(Suppl):163-172.

Kornreich F. Identification of best electrocardiographic leads for diagnosing acute myocardial ischemia. J Electrocardiol 1998; 31(Suppl):157-163.

Kors JA, Ritsema van Eck HJ, van Herpen G. The U wave explained as an intrinsic part of repolarization. Computers in Cardiology 2005; 32:101-104.

Kors JA, de Bruyne MC, Hoes AW, van Herpen G, Hofman A, van Bemmel JH, Grobbee DE. T axis as an indicator of risk of cardiac events in elderly people. Lancet 1998;352:601-605.

Kors JA, van Herpen G, van Bemmel JH. QT dispersion as an attribute of T-loop morphology. Circulation 1999; 99:1458-1463.

Krone RJ, Friedman E, Thanavaro S, Miller JP, Kleiger Re, Oliver GC. Long-term prognosis after first Q-wave (transmural) or non-Q-wave (nontransmura) myocardial infarction: Analysis of 593 patients. Am J Cardiol 1983;52:234-239.

Kubota I, Hanashima K, Ikeda K, Tsuiki K, Yasui S. Detection of diseased coronary artery by exercise ST-T maps in patients with effort angina pectoris, single-vessel disease, and normal ST-T wave on electrocardiogram at rest. Circulation 1989;80:120-127.

Kubota I, Ideka K, Kanaya T, Yamaki M, Tonooka I, Watanabe Y, Tsuiki K, Yasui S. Noninvasive assessment of left ventricular wall motion abnormalities by QRS isointegral maps in previous anterior infarction. Am Heart J 1985:109: 464-471.

Langer, A. Goodman, S G. Topol, E J. Charlesworth, A. Skene, A M. Wilcox, R G. Armstrong, P W. Late assessment of thrombolytic efficacy (LATE) study: prognosis in patients with non-Q wave myocardial infarction. (LATE Study Investigators). J Am Coll Cardiol 1996;27:1327-32.

Lee HS, Cross SJ, Rawles JM, Jennings KP. Patients with suspected myocardial infarction who present with ST depression. Lancet 1993; 342:1204-07.

Liu G, Iden JB, Kovithavongs K, Gulanhusein R, Duff HJ, Kavanagh K. In vivo temporal and spatial distribution of depolarization and repolarization and the illusive murine T wave. The Journal of Physiology 2003; 555:267-279.

Lux RL, Urie PM, Burgess MJ, Abildskov JA. Variability of the body surface distributions of QRS, ST-T and QRST deflection areas with varied activation sequence in dogs. Cardiovascular Research 1980;14:607-12.

MacFarlane P. The normal electrocardiogram and vectorcardiogram. In: Comprehensive Electrocardiology. MacFarlane P, Lawrie TD, Eds. Vol 3, Pergamon press 1989a: 452-455.

MacFarlane P. Coding schemes. In Comprehensive Electrocardiology. MacFarlane P, Lawrie TD, Eds. Vol 3, Pergamon press 1989b: 1567-1582.

MacLeod RS, Gardner M, Miller RM, Horacek BM. Application of an electrocardiographic inverse solution to localize ischemia during coronary angioplasty. J Cardiovasc Electrophysiol 1995;6:2-18.

MacLeod RS, Lux RL, Taccardi B. A possible mechanism for electrocardiographically silent changes in cardiac repolarization. J Electrocardiol 1998; 30 (Suppl):114-21.

Malik M, Acar B, Gang Y, Yap YG, Hnatkova K, Camm AJ. QT dispersion does not represent electrocardiographic interlead heterogeneity of ventricular repolarization. J Cardiovasc Electrophysiol 2000;11:835-843.

Malik M. Hnatkova K. Batchvarov VN. Post infarction risk stratification using the 3-D angle between QRS complex and T-wave vectors. Journal of Electrocardiology. 37 Suppl:201-8, 2004.

Marcus EB, Yano K, MacLean CJ. Regression of Q waves following acute myocardial infarction. American Journal of Epidemiology 1989;129:105-111.

Maynard SJ, Menown IB, Manoharan G, Allen J, McC Anderson J, Adgey AAJ. Body surface mapping improves early diagnosis of acute myocardial infarction in patients with chest pain and left bundle branch block. Heart 2003; 89:998-1002.

Maynard SJ, Riddell JW, Menown IB, Allen J, Anderson JM, Khan MM, Adgey AA. Body surface potential mapping improves detection of ST segment alteration during percutaneous coronary intervention. Int J Cardiol 2004;93:203-10.

McClelland A, Owens C, Menown I, Lown M, Adgey J. Comparison of the 80-lead body surface Map to physician and to 12-lead electrocardiogram in detection of acute myocardial infarction. Am J Cardiol 2003:92: 252-257.

McMechan SR, Cullen CM, MacKenzie G, Dempsey GJ, Wright GT, Crawley M, Anderson J, Adgey AA. Discriminant function analysis of body surface potential maps in acute myocardial infarction. J Electrocardiol 1994; (27 Suppl):117-20.

McMechan SR, MacKenzie G, Allen J, Wright GT, Dempsey GJ, Crawley M, Anderson J, Adgey AA. Body surface ECG potential maps in acute myocardial infarction. J Electrocardiol 1995; 28 Suppl:184-90.

McPherson DD, Horacek BM, Spencer CA, Johnstone DE, Lalonde LD, Cousins CL, Montague TJ. Indirect measurement of infarct size: correlative variability of enzyme, radionuclear angiographic and body surface map variables in 34 patients during the acute phase of first myocardial infarction. Chest 1985; 88:841-848.

Medvegy M, Duray G, Pinter A, Preda I. Body surface potential mapping:Historical bacground, present possibilities, diagnostic challenges. Ann Noninvasive Electrocardiol 2002; 7:139-151.

Medvegy M, Preda I, Savard P, Pinter A, Tremblay G, Nashmith J, Palisatis D, Nadeau R. New body surface isopotential map evaluation method to detect minor potential losses in non-Q-wave myocardial infarction. Circulation 2000:101: 1115-1121.

Menown I, Allen J, McC Anderson J. Adgey A. ST depression only on the initial 12-lead ECG: early diagnosis of acute myocardial infarction. Eur Heart J 2001:22: 218-227.

Menown IB, Allen J, Anedrson JM, Adgey AA. Noninvasive assessment of reperfusion after fibrinolytic therapy for acute myocardial infarction. Am J Cardiol 2000; 86:736-41.

Menown IB, MacKenzie G, Adgey AA. Opitmizing the initial 12-lead electrocardiographic diagnosis of acute myocardial infarction. Eur Heart J;2000:21:275-83.

Menown IBA, Allen J, Anderson JM, Adgey AAJ. Early diagnosis of right ventricular or posterior infarction associated with inferior wall left ventricular acute myocardial infarction. Am J Cardiol 2000; 85:934-8.

Menown IBA, Patterson RSHW, MacKenzie G, Adgey AAJ. Body surface map models for early diagnosis of acute myocardial infarction. J Electrocardiol 1998; 31(Suppl):180-187.

Mirvis DM, Ingram L, Holly MK, Wilson JL, Ramanathan KB. Electrocardiographic effects of experimental nontransmural myocardial infarction. Circulation 1985; 71:1206-14

Mirvis DM. Current status of body surface electrocardiographic mapping. Circulation 1987; 75:684-688.

Mirvis DM. Physiologic bases for anterior ST-segment depression in patients with acute inferior wall myocardial infarction. Am Heart J 1988; 116:1308-1322.

Montague T, Smith E, Spencer CA, Johnstone DE, Lalonde LD, Bessoudo RM, Gardner MJ, Anderson RN, Horacek BM. Body surface electrocardiographic mapping in inferior myocardial infarction. Manifestation of left and right ventricular involvement. Circulation 1983:67: 665-673.

Montague TJ, Johnstone DE, Spencer CA, Lalonde LD, Gardner MJ, O'Reilly MG, Horacek BM. Non-Q-wave myocardial infarction: Body surface potential map and ventriculographic patterns. Am J Cardiol 1986:58: 1173-1180.

Montague TJ, McPherson DD, Johnstone DE, Spencer C, Lalonde L, Gardner M, Horacek B. Electrocardiographic and ventriculographic recovery patterns in Q wave myocardial infarction. J Am Coll Cardiol 1986:8: 521-528.

Montague TJ, Smith ER, Cameron DA, Rautaharju PM, Klassen GA, Felmington CS, Horacek BM. Isointegral analysis of body surface maps: Surface distribution and temporal variability in normal subjects. Circulation 1981;63:116-1172.

Montague TJ, Smith ER, Johnstone DE, Spencer CA, Lalonde LD, Bessoudo RM, Gardner MJ, Anderson RN, Horaeck BM. Temporal evolution of body surface map patterns following acute inferior myocardial infarction. J Electrocardiol 1984; 17:319-27.

Montague TJ, Witkowski FX. The clinical utility of body surface potential mapping in coronary artery disease. Am J Cardiol 1989;64:378-383.

Moon JCC, Perez De Arenaza D, Elkington AG, Taneja AK, John AS, Wang D, Janardhanan R, Senior R, Lahiri A, Poole-Wilson PA, Pennell DJ. The pathologic basis of Q-wave and non-Q-wave myocardial infarction: a cardiovascular magnetic resonance study. J Am Coll Cardiol 2004; 44:554-60.

Nakajima T, Kowakubo K, Toda I, Mashima S, Ohtake T, Iio M, Sugimoto T. ST-T isointegral analysis of exercise stress body surface mapping for identifying ischemic areas in patients with angina pectoris. Am Heart J 1988; 115:1013-1020.

Nash MP, Bradley CP, Paterson DJ. Imaging electrocardiographic dispersion of depolarization and repolarization during ischemia: Simultaneous body surface and epicardial mapping. Circulation 2003;107:2257-2263.

Nishiyama A, Suzuki A, Hayashi H, Shimizu S, Watarai M, Saito M, Shiga Y, Furuta T, Takatsu F, Adachi M, et al. Comparative study of QRST values from body surface potential mapping, 12-lead ECGs, VCGs in detecting inferior myocardial infarction, and evaluating the severity of left ventricular wall motion abnormalities in simulated left bundle branch block. J Electrocardiol 1993;26:18-96.

Noble D, Cohen IS. The interpretation of the T wave of the electrocardiogram. Cardiovasc Res 1978; 12:13-27.

Oikarinen L, Karvonen M, Viitasalo M, Takala P, Kaartinen M, Rossinen J, Tierala I, Hänninen H, Katila T, Nieminen M, Toivonen L. Electrocardiographic assessment of left ventricular hypertrophy with time-voltage QRS and QRST-wave areas. Journal of Human Hypertension 2004;18, 33-40.

Oikarinen L, Karvonen M, Viitasalo M, Takala P, Kaartinen M, Rossinen J, Tierala I, Hänninen H, Katila T, Nieminen MS, Toivonen L. Electrocardiographic assessment of left ventricular hypertrophy with time-voltage QRS and QRST-wave areas. Journal of Human Hypertension 2004;18:33-40.

Ornato JP, Menown IBA, Riddell JW, Carley S, Mackway-Jones K, Higgins GL, et al. 80-lead body map detects acute ST-segment elevation myocardial infarction missed by standard 12-lead electrocardiography. J Am Coll Cardiol 2002; 39:332A.

Osugi J, Ohta T, Toyama J, Takatsu F, Nagaya T, Yamada K. Body surface isopotential maps in old inferior myocardial infarction undetectable by 12-lead electrocardiogram. J Electrocardiol 1984; 17:55-62.

Owens CG, McClelland AJ, Walsh SJ, Smith BA, Tomlin A, Riddel JW, Stevenson M, Adgey AA. Prehospital 80-LAD mapping: does it add significantly to the diagnosis of acute coronary syndromes? J Electrocardiol 2004; 37 (Suppl):223-32.

Pahlm O, Haisty WK, Wagner NB, Pope JE, Wagner GS. Specificity and sensitivity of QRS criteria for diagnosis of single and multiple myocardial infarcts. Am J Cardiol 1991;68:1300-1304.

Pahlm US, Chaitman BR, Rautaharju PM, Selvester RH, Wagner GS. Comparison of the various electrocardiographic scoring codes for estimating anatomically documented sizes of single and multiple infarcts of the left ventricle. Am J Cardiol 1998;81:809-815.

Palmeri ST, Harrison DG, Cobb FR, Morris KG, Harrell FE, Ideker RE, Selvester RH, Wagner GS. A QRS scoring system for assessing left ventricular function after myocardial infarction. NEJM 1982;306:4-9.

Pardee HEB. An electrocardiographic sign of coronary artery obstruction. Arch Intern Med 1920; 26:244-257.

Perin EC, Silva GV, Sarmento-Leite R, Sousa ALS, Howell M, Muthupillai R, Lambert B, Vaughn WK, Flamm S. Assessing myocardial viability and infarct transmurality with left ventricular electromechanical mapping in patients with stable coronary artery

disease. Validation by delayed-enhancement magnetic resonance imaging. Circulation 2002; 106:957-961.

Pipberger HV, Simonson E, Lopez EA, Araoye MA, Pipberger HA. The electrocardiogram in epidemiologic investigations. A new classification system. Circulation 1982;65:1465-1464.

Prineas RJ, Grandits G, Rautaharju PM, Cohen JD, Zhang ZM, Crow RS, for the MRFIT Research Group. Long-term prognostic significance of isolated minor electrocardiographic T-wave abnormalities in middle-aged men free of clinical cardiovascular disease (The Multiple Risk Factor Intervention Trial [MRFIT]). Am J Cardiol 2002;90:1391-1395.

Raunio H, Rissanen V, Romppanen T, Jokinen Y, Rehnberg S, Helin M, Pyörälä K. Changes in the QRS complex and ST segment in transmural and subendocardial MIs: a clinico-pathological study. Am Heart J 1979; 98:176-84.

Rautaharju PM, Clark Nelson J, Kronmal RA, Zhang ZM, Robbins J, Gottdiener JS, Furberg CD, Manolio T, Fried L. Usefulness of T-axis deviation as an independent risk indicator for incident cardiac events in older men and women free from coronary heart disease (The Cardiovascular Health Study). Am J Cardiol 2001; 88:118-123.

Rautaharju PM, Warren JW, Jain U, Wolf HK, Nielsen CL. Cardiac Infarction Injury Score: An electrocardiographic coding scheme for ischemic heart disease. Circulation 1981;64:249-256.

Rosenbaum MB, Blanco HH, Elizari MV, Lazzari JO, Davidenko JM. Electrotonic modulation of the T wave and cardiac memory. Am J Cardiol 1982;50:213-22.

Savonitto S, Ardissino D, Granger CB, Morando G, Prando MD, Mafrici A, Cavallini C, Melandri G, Thompson TD, Vahanian A, Ohman EM, Califf RM, Van de Werf F, Topol EJ. Prognostic Value of the Admission Electrocardiogram in Acute Coronary Syndromes. J Am Med Assoc.1999;281:707-713.

Self WH, Mattu A, Martin M, Holstege C, Preuss J, Brady WJ. Body surface mapping in the ED evaluation of the patient with chest pain: use of the 80-lead electrocardiogram system. American Journal of Emergency Medicine 2006; 24:87-112.

Selvester RH, Wagner GS, Hindman NB. The Selvester QRS scoring system for estimating myocardial infarct size. The development and application of the system. Arch Intern Med 1985:145:1877-1881.

Sevilla D, Wagner N, Pegues R, Peck S, Mikat E, Ideker R, Hutchins G, Reimer K, Hackel D, Selvester R, Wagner G. Correlation of the complete version of the Selvester QRS scoring system with quantitative anatomic findings for multiple left ventricular myocardial infarcts. Am J Cardiol 1992;69:465-469.

Sheifer SE, Manolio T, Gersh BJ. Unrecognized myocardial infarction. Ann Intern Med 2001;135:801-811.

Sicouri S, Antzelevitch C. A subpopulation of cells with unique electrophysiological properties in the deep subepicardium of the canine ventricle: The M cell. Circ Res 1991; 68:1729-1741.

Sievers B, John B, Brandts B, Franken U, van Bracht M, Trappe HJ. How reliable is electrocardiography in differentiating transmural from non-transmural myocardial infarction? A study with contrast magnetic resonance imaging as gold standard. International Journal of Cardiology 2004;97:417-423.

Sigurdsson E, Thorgeirsson G, Sigvaldsson H, Sigfusson N. Unrecognized myocardial infarction:epidemiology, clinical characteristics, and the prognostic role of angina pectoris. The Reykjavik Study. Annals of Internal Medicine 1995:122:96-102.

Simson MB. Signal-averaged electrocardiography. Cardiac Electrophysiology. From cell to bedside. Edited by Zipes DP and Jalife J. Philadelphia, WB Saunders, 1990.

Sokolow M, Lyon T. The ventricular complex in left ventricular hypertrophy as obtained by unipolar precordial and limb leads. Am Heart J 1949;37:161.

Speake D, Polly T. First ECG in chest pain. Emerg Med J 2001; 18:61-62.

Surawicz B. Resting membrane potential, action potential, and passive membrane properties. In: Electrophysiological basis of ECG and cardiac arrhytmias. Williams and Wilkins, Philadelphia 1995:25-39.

Surawicz B. Spread of activation in the heart. In: Electrophysiologic basis of ECG and cardiac arrhythmias. Williams & Wilkins, Philadelphia 1995, pp. 257-267.

Surawicz B. Electrocardiographic theory and methods of recording. In: Electrophysiological basis of ECG and cardiac arrhytmias. Williams and Wilkins, Philadelphia 1995:493-506.

Surawicz B. Spread of activation in the heart. In: Electrophysiologic basis of ECG and cardiac arrhythmias. Williams & Wilkins, Philadelphia 1995, pp. 556-557.

Terkelsen CJ, Norgaard BL, Lassen JF, Poulsen SH, Gerdes JC, Sloth E, Gotzsche LB, Romer FK, Thuesen L, Nielsen TT, Andersen HR. Potential significance of spontaneous and interventional ST-changes in patients transferred for primary percutaneous coronary intervention: observations fro the ST-MONitoring in Acute Myocardial Infarction study (The MONAMI study). Eur Heart J 2006; 27:267-275.

Thygesen K, Alpert JS. The Joint European Society of Cardiology/American College of Cardiology Committee. Myocardial infarction redefined - A consensus document of The Joint European Society of Cardiology/American College of Cardiology Committee for the Redefinition of Myocardial Infarction. Eur Heart J 2000;21:1502-1513/J Am Coll Cardiol 2000; 36:959-969.

TIMI IIIB Investigators. Effects of tissue plasminogen activator and a comparison of early invasive and conservative strategies in unstable angina and non Q-wave myocardial infarction. Results of the TIMI IIIB trial. Circulation 1994;89:1545-56.

Tonooka I, Kubota I, Watanabe Y, Tsuiki K, Yasui S. Isointegral analysis of body surface maps for the assessment of location and size of myocardial infarction. Am J Cardiol 1983;52:1174-1180.

Tseng YZ, Hsu KL, Chiang FT, Lo HM, Hwang JJ, Lai LP, Lin JL, Tseng CD. Characteristic findings of body surface potential map during ventricular repolarization in patients with coronary heart disease. Jpn Heart J 1999; 40:391-404.

Tsunakawa H, Hoshino K, Kanesaka S, Harumi K, Okamoto Y, Teramachi Y, Musha T. Dipolarity and dipole location during QRS and T waves in normal men estimated from body surface potential distribution. Jpn Heart J. 1985; 26:319-334.

Uusitupa M, Pyörälä K, Raunio H, Rissanen V, Lampainen E. Sensitivity and specificity of Minnesota code Q-QS abnormalities in the diagnosis of myocardial infarction verified at autopsy. Am Heart J 1983;106:753-757.

Wagner GS, Maynard C, Andersen A, Anderson E, Myers R, Warner RA, Selvester RH. Evaluation of advanced electrocardiographic diagnostic software for detection of prior myocardial infarction. Am J Cardiol 2002; 89:75-79.

Walker SJ, Bell AJ, Loughhead MG, Lavercombe PS, Kilpatrick D. Spatial distribution and prognostic significance of ST segment potential determined by body surface mapping in patients with acute inferior myocardial infarction. Circulation 1987; 76:289-297.

Van de Werf F, Ardissino D, Betriu A, Cokkinos DV, Falk E, Fox KAA, Julian D, Lengyel M, Neumann F-J, Ruzyllo W, Thygesen C, Underwood SR, Vahanian A, Verheugt FWA, Wijns W. Management of acute myocardial infarction in patients presenting with ST-segment elevation. The Task Force on the Management of Acute Myocardial Infarction of the European Society of Cardiology. Eur Heart J 2003; 24:28-66.

Van't Hof AW, Liem A, de Boer MJ, Zijlstra F. Clinical value of 12-lead electrocardiogram after successful reperfusion therapy for acute myocardial infarction. Zwolle Myocardial Infarction Study Group. Lancet 1997; 350:615-619.

Warner RA, Hill NE, Lynch T. Usefulness of abnormalities of repolarization in the electrocardiographic diagnosis of healed myocardial infarction. J Electrocardiol 1988 (Suppl):93-97.

Willems JL, Abreu-Lima C, Arnaud P, van Bemmel JH, Brohet C, Degani R, Denis B, Gehring J, Graham I, van Herpen G, Machado H, Macfarlane PW, Michaelis J, Moulopoulos S, Rubel P, Zywietz C. The diagnostic performance of computer programs for the interpretation of electrocardiograms. N Engl J Med 1991; 325:1767-73.

Wilson FN, Macleod AG, Barker PS, Johnston FD. Determination and the significance of the areas of the ventricular deflections of the electrocardiogram. Am Heart J.1934;10:46-61.

Vincent GM, Abildskov JA, Burgess MJ. Mechanisms of ischemic ST-segment displacement. Evaluation by direct current recordings. Circulation 1977;56:559-566.

Von Essen RV, Merx W, Doerr R, Effert S, Silny J, Rau G. QRS mapping in the evaluation of acute anterior myocardial infarction. Circulation 1980; 62:266-76.

Wong C-K, Stewart RAH, Gao W, French JK, Raffel OC, White HD, for the Hirulog and Early Reperfusion or Occlusion (HERO-2) Trial Investigators. Prognostic differences between different types of bundle branch block during the early phase of acute myocardial infarction: insights from the Hirulog and Early Reperfusion or Occlusion (HERO-2) trial. Eur Heart J 2006; 27:21-28.

World Health Organization Task Force on Standardisation of Clinical Nomenclature: Nomenclature and criteria for diagnosis of ischaemic heart disease. Circulation 1979; 59: 607-609.

Yamashita Y. Theoretical studies on the inverse problem in electrocardiography and the uniqueness of the solution. IEEE Trans Biomed Eng 1982;BME-29:719-725.

Yan GX, Antzelevitch C. Cellular basis for the normal T wave and the electrocardiographic manifestations of the long QT syndrome. Circulation 1998; 98:1928-36.

Yang H, Pu M, Rodriguez D, Underwood D, Griffin BP, Kalahasti V, Thomas JD, Brunken RC. Ischemic and viable myocardium in patients with non-Q-wave or Q-wave myocardial infarction and left ventricular dysfunction: a clinical study using positron emission tomography, echocardiography, and electrocardiography. J Am Coll Cardiol 2004;43:592-8.

Yano K, MacLean CJ. The incidence and prognosisi of unrecognized myocardial infarction in the Honolulu, Hawaii Heart Program. Arch Intern Med 1989; 149:1528-32.

Yuan S, Kongstad O, Hertervig E, Holm M, Grins E, Olsson B. Global repolarization sequence of the ventricular endocardium: Monophasic action potential mapping in swine and humans. PACE 2001; 24:1479-1488.

Zabel M, Acar B, Klingenheben T, Franz MR, Hohnloser SH, Malik M. Analysis of 12-lead T-wave morphology for risk stratification after myocardial infarction. Circulation 2000; 102:1252-1257.

Zabel M, Malik M, Hnatkova K, Papademetriou V, Pittaras A, Fletcher RD, Franz MR. Analysis of T-wave morphology from the 12-lead electrocardiogram for prediction of long-term prognosis in male US veterans. Circulation 2002; 105:1066-1070.